

# Microbial metabolic rates in the Ross Sea: the ABIOCLEAR Project

Maurizio Azzaro<sup>1</sup>, Theodore T. Packard<sup>2</sup>, Luis Salvador Monticelli<sup>1</sup>,  
Giovanna Maimone<sup>1</sup>, Alessandro Ciro Rappazzo<sup>1,3</sup>, Filippo Azzaro<sup>1</sup>, Federica  
Grilli<sup>4</sup>, Ermanno Crisafi<sup>1</sup>, Rosabruna La Ferla<sup>1</sup>

**1** Institute of Polar Science (ISP-CNR Messina), Spianata S. Raineri 86, 98122 Messina, Italy **2** Marine Ecophysiology Group (EOMAR), University of Las Palmas de Gran Canaria, Campus Universitario de Tafira 35017, Las Palmas de Gran Canaria, Spain **3** National Interuniversity Consortium for Marine Sciences (CO-NISMa), Piazzale Flaminio 9, 00196 Roma, Italy **4** Institute for Biological Resources and Marine Biotechnologies (IRBIM-CNR Ancona), Largo Fiera della Pesca 2, 60125 Ancona, Italy

Corresponding author: Rosabruna La Ferla ([rosabruna.laferla@cnr.it](mailto:rosabruna.laferla@cnr.it))

---

Academic editor: A. Lugliè | Received 17 October 2018 | Accepted 25 February 2019 | Published 3 May 2019

---

<http://zoobank.org/83471DD2-4EB3-4F6F-A8FA-B02F7117115>

---

**Citation:** Azzaro M, Packard TT, Monticelli LS, Maimone G, Rappazzo AC, Azzaro F, Grilli F, Crisafi E, La Ferla R (2019) Microbial metabolic rates in the Ross Sea: the ABIOCLEAR Project. In: Mazzocchi MG, Capotondi L, Freppaz M, Lugliè A, Campanaro A (Eds) Italian Long-Term Ecological Research for understanding ecosystem diversity and functioning. Case studies from aquatic, terrestrial and transitional domains. Nature Conservation 34: 441–475. <https://doi.org/10.3897/natureconservation.34.30631>

---

## Abstract

The Ross Sea is one of the most productive areas of the Southern Ocean and includes several functionally different marine ecosystems. With the aim of identifying signs and patterns of microbial response to current climate change, seawater microbial populations were sampled at different depths, from surface to the bottom, at two Ross Sea mooring areas southeast of Victoria Land in Antarctica. This oceanographic experiment, the XX Italian Antarctic Expedition, 2004-05, was carried out in the framework of the ABIOCLEAR project as part of LTER-Italy. Here, microbial biogeochemical rates of respiration, carbon dioxide production, total community heterotrophic energy production, prokaryotic heterotrophic activity, production (by <sup>3</sup>H-leucine uptake) and prokaryotic biomass (by image analysis) were determined throughout the water column. As ancillary parameters, chlorophyll *a*, adenosine-triphosphate concentrations, temperature and salinity were measured and reported. Microbial metabolism was highly variable amongst stations and depths. In epi- and mesopelagic zones, respiratory rates varied between 52.4–437.0 and 6.3–271.5 nM O<sub>2</sub> l<sup>-1</sup> h<sup>-1</sup>; prokaryotic heterotrophic production varied between 0.46–29.5 and 0.3–6.11 nM C l<sup>-1</sup> h<sup>-1</sup>; and prokaryotic biomass varied between 0.8–24.5 and 1.1–9.0 μg C l<sup>-1</sup>, respectively. The average heterotrophic energy production ranged between 570 and 103 mJ l<sup>-1</sup> h<sup>-1</sup> in upper

and deeper layers, respectively. In the epipelagic layer, the Prokaryotic Carbon Demand and Prokaryotic Growth Efficiency averaged 9 times higher and 2 times lower, respectively, than in the mesopelagic one. The distribution of plankton metabolism and organic matter degradation was mainly related to the different hydrological and trophic conditions. In comparison with previous research, the Ross Sea results, here, evidenced a relatively impoverished oligotrophic microbial community, throughout the water column.

### Keywords

Microbial respiration, heterotrophic production, heterotrophic energy production, Ross Sea, Antarctica, LTER

### Introduction

The present work aims to explore the carbon fate through microbes in an area of the Ross Sea (RS) and to identify signs and patterns of microbial responses to current climate change.

The Southern Ocean (SO) plays an important role in world climate since it is considered the engine of the worldwide oceanic currents. The dramatic seasonal variability in environmental factors in SO generates a significant stress on the biota which must endure constant sunlight, oscillating temperatures and melting ice phenomena in spring-summer time. The annual pelagic primary production is largely confined to this period, when light and nutrient conditions are favourable for the phytoplankton growth. Studies on global change have revealed that the SO is becoming a larger carbon sink with over 30–40% of total carbon uptake occurring there (Lancelot 2007, Khatiwala et al. 2009). Recently, an early spring retreat of sea ice, along with a decrease in seasonal sea-ice cover, an increase of light availability and a presumed constraint on primary production, has also been reported (Dinasquet et al. 2018, Constable et al. 2014). Furthermore, the low iron-limited primary productivity ensures that SO falls into a high-nutrient low-chlorophyll (HNLC) type of environment (Minas et al. 1986, Dinasquet et al. 2018, Deppler and Davidson 2017).

One of the most productive and peculiar area of the SO continental shelf zone is the RS (Nelson et al. 1996). This region (1.55 million km<sup>2</sup> of ocean bordering Antarctica from ice edge to deep ocean) was established as a Marine Protected Area (MPA) in December 2017. Here, a peculiar and relatively simple trophic web exists. The phytoplankton, dominated by either diatoms or *Phaeocystis* sp., depending on whether the euphotic zone is stratified or deeply mixed, is grazed either by krill or silver fish that, in turn, sustain the higher trophic levels (Deppler and Davidson 2017). The RS includes a mosaic of functionally different marine ecosystems mainly linked to sea ice distribution whose variability induces unpredicted cascade effects on trophic dynamics and carbon and nutrient drawdown (Catalano et al. 2006, Smith et al. 2007, Vichi et al. 2009). Accordingly, different fates involve the organic matter transfer, carbon export and depth sequestration. The relevance of high latitude oceans, such as the RS, to models and budgets of global carbon cycling has stimulated recent studies of organic matter degradation in the RS water column (Nelson et al. 1996, Carlson and Hansell 2003, Langone et al. 2003, Azzaro et al. 2006, Misic et al. 2017).

Catalano et al. (2006) confirmed that, in spring-summer periods, about 90% of the total carbon derived from new production was exported *via* higher trophic levels. Comparing the oxidation and sinking of organic matter through the deep water found that, according to sediment-traps estimates, 63% of organic carbon, remineralized to CO<sub>2</sub> by microbial respiration, originated in the particulate organic matter (*POC*) pool (Azzaro et al. 2006). Such evidence highlighted *POC* as the main organic fuel in the RS biological pump. The oxidation rate, fuelling the dissolved organic fraction, was not measured by sediment traps (Jiao et al. 2010, Legendre et al. 2015), but it was a smaller fraction, here in the RS, than it was in other oceans (Azzaro et al. 2006).

Although microbes constitute the sentinel of ecosystem evolution (Dutta and Dutta 2016), to date, relatively little is known in the RS about the microbial contribution to the degradation of the carbon pool. Amongst the biological processes and metabolic activities, respiration has particularly been neglected despite its great impact on environmental ecology (Packard 2017). Respiration is controlled by the respiratory electron transport system activity (*ETS*) in all organisms on the planet (Packard 1969, Packard et al. 1971, Lane 2006, Packard et al. 2015). It functions in aerobic and anaerobic conditions, as well as in extreme or deep marine environments (Koppelman et al. 2004, Azzaro et al. 2006, Packard and Codispoti 2007, Baltar et al. 2010). The *ETS* assay was originally designed by Packard (1971). The biochemical relationship amongst the biological energy currency, adenosine triphosphate (*ATP*) and *ETS* was completely unknown before the 1940s. In few words, in all living organisms, during cellular respiration, the electron transport system produces the bulk of the cell energy in the form of *ATP* molecules. However, earlier, the idea of capturing biologically usable energy from respiration was appreciated by the biophysicist, Alfred Lotka (1925). He felt that Darwinian natural selection was the result of competition between organisms for energy. Those individuals that extracted, stored and used energy most efficiently survived and reproduced more often than their competitors. Building on this concept, Howard Odum described energy flow in freshwater streams (Odum 1956). David Karl recently argued that biological energy production in the ocean should be assessed to understand ocean productivity better (Karl 2014).

Still, none of the earlier work calculated energy production from the biochemical processes that produce this energy. They used distantly related proxies such as biomass or, the more related one, heat production (Pamatmat et al. 1981). Here, we calculate the heterotrophic side of biological energy production (*HEP*) in the RS. *HEP* is the *ATP* generation that results from protons being pumped across the prokaryote plasmalemma or the eukaryote mitochondrial inner membrane by the respiratory *ETS*. This pumping stores energy in the form of a proton gradient across these membranes. It is manifest as both a hydrogen-ion gradient, with a pH change across the membrane as high as 1 pH unit (Procopio and Fornés 1997) and a voltage gradient with an electromotive force (EMF), equal to 170–225 mV. Both cross-membrane gradients, when there is no electron or proton leakage, generate a force across the membrane that is equal to the EMF in millivolts. These gradients, above about 225 mV, force protons back across the membrane, through the molecular motor, *ATP* synthetase (EC 3.6.3.14), to catalyse

the phosphorylation of *ADP* to *ATP* ( $ADP + \text{Pi} + \text{H}^+_{\text{out}} \rightleftharpoons ATP + \text{H}_2\text{O} + \text{H}^+_{\text{in}}$ ) (Berg et al. 2002). This is the main way by which heterotrophic organisms produce their energy. The biochemistry of the connection between *ATP* and the *ETS* was poorly known until the Nobelist, Severo Ochoa, determined how three *ATP* molecule were produced for every oxygen atom (P/O ratio) used in respiratory oxygen consumption (Ochoa 1943). A decade later, Odum (1956) described energy flow in fresh water streams. Much later, working with the copepod *Acartia tonsa*, Dana 1849, Kiørboe et al. (1985) used modern biochemical understanding of the relationship between respiration and oxidative phosphorylation to calculate *ATP* production during growth and egg production. In this millenium, Karl (2014), cognisant of Odum's thinking, as well as the ocean research of Holm-Hansen and Booth (1966) and Packard et al. (1971), advocated assessing biological energy production in the ocean to help understand regional differences in primary productivity. Here and in Packard et al. (2015), we build on this reasoning to calculate *HEP* and the *ATP* turnover rate for the seawater of the RS. This *HEP* is *ATP* produced by respiratory  $\text{O}_2$  consumption ( $\text{RO}_2$ ) both in the epipelagic microplankton community of phytoplankton, prokaryotes and protozoans and in the mesopelagic microplankton communities of prokaryotes and protozoans.

In order to analyse the role of prokaryotic metabolism as a regulator of the organic carbon budget, seawater samples were taken in a quadrilateral area of the RS where four mooring sites were located. Fifteen stations were sampled in the epipelagic layer (from surface to 100 m) and in the mesopelagic one (from > 100 m to 800 m) to broaden the evaluation of the whole area.

The prokaryotic biomass (*PB*) was detected by Image Analysis cell counts and volume measurements. The *ETS* assay was adopted to calculate respiration rates of microplankton (< 200  $\mu\text{m}$ ) in terms of oxygen utilisation (*OUR*), carbon dioxide production (*CDPR*) rates and heterotrophic energy production (*HEP*). In some stations, the prokaryotic heterotrophic activity and the heterotrophic carbon production by  $^3\text{H}$ -leucine uptake (*PHA* and *PHP*, respectively) were measured. Ancillary parameters were chlorophyll *a* (*CHLa*), adenosine triphosphate (*ATP*) concentrations and the hydrological parameters. We tried to simultaneously analyse the bulk C metabolism of prokaryotic assemblage, by direct measurement of different independent parameters (respiration and heterotrophic production) and their interconnections (*HEP*, *PCD* and *PGE*).

The aims of the paper were 1) to monitor the role of microbes as regulators of the organic carbon transfer in the biogeochemical processes, 2) to compare the obtained data with other surveys in RS and 3) to use microbial respiratory and metabolic activity patterns as proxies to describe microbial ecosystem trends.

## Methods

During the XX Italian PNRA (National Programme of Antarctic Research, year 2004/05) expedition, in the framework of the ABIOCLEAR project (Antarctic BIOgeochemical cycles-CLimatic and palEoclimAtic Reconstructions), an oceanographic cruise was carried out from 4 January to 14 February 2005 aboard the Italian R/V *Italica*. In a quadrilateral

area between four mooring sites (mooring A and B, monitored in the framework of LTER-Italy activity in Antarctica and moorings H and D), a total of fifteen stations were sampled throughout the water column, from surface to 800 m depth, using a Rosette sampler with 24, 12 l, Niskin bottles. The Rosette was mounted on a CTD equipped with a Sea-Bird 9/11 plus multiparametric probe (SeaBird Electronics) that sensed temperature ( $T$ ), conductivity (salinity,  $S$ ) and dissolved oxygen ( $DO$  [SBE 43]). In Figure 1, the map of the sampling area and in Table 1, the names of stations, their coordinates, maximum depths and studied parameters are reported. In Suppl. material 2: Table S1, the acronyms of the studied parameters and the link amongst some of them are reported.

### Trophic measurements (ATP and CHLa)

For  $ATP$  measurements, 1 l of seawater was prefiltered through a 250  $\mu\text{m}$  net and then filtered through a 0.22  $\mu\text{m}$  membrane filter. The filter was immediately plunged into 3 ml boiling TRIS–EDTA phosphate buffer (pH 7.75) and the  $ATP$  was extracted at 10 °C for 3 min and kept frozen (-20 °C) until laboratory analysis in Italy (Holm-Hansen and Paerl 1972). The filtrate, from the  $ATP$  sample, was stored in sterile polycarbonate bottles. Extracts for  $ATP$  determination were prepared according to Holm-Hansen and Paerl (1972) and analysed by measuring the peak height of the firefly bioluminescence with a Lumat LB9507 luminometer by EG&G Berthold. The conversion factor,  $C/ATP = 250$ , was adopted to convert  $ATP$  values into carbon biomass units ( $C-ATP$ ) according to Karl (1980). The accuracy of this conversion is  $\pm 20\%$  (Skjoldal and Båmstedt 1977). According to  $ATP$  concentrations, Karl (1980) classified the trophic status of marine systems as follows: oligotrophy when  $ATP$  is  $< 100 \text{ ng l}^{-1}$ ; moderate trophism  $ATP > 100 < 500 \text{ ng l}^{-1}$  and eutrophy  $ATP < 500 \text{ ng l}^{-1}$ .

$CHLa$  concentrations, as an index of phytoplankton biomass, were determined in the water column from surface to a maximum of 160 m depth. The water samples (1 l) were filtered on Whatman GF/F glass-fibre filters, according to Lazzara et al. (1990). After filtration, the filters were immediately stored at -20 °C.  $CHLa$  was extracted in 90% acetone and read before and after acidification. Determinations were carried out with a Varian Eclipse spectrofluorometer. Maximum excitation and emission wavelengths (431 and 667 nm, respectively) were selected on a pre-scan with a solution of  $CHLa$  from *Anacystis nidulans* (Sigma-Aldrich Co). The conversion factor of  $C-CHL = 100$  was adopted to convert  $CHLa$  values into carbon biomass units (Smith et al. 1998).

The Trophic State Index ( $TSI$ ), applied to classify the stations according to their algal biomass, was calculated from the chlorophyll measurements (Carlson 1983:  $TSI (CHLa) = 9.81 \ln(CHLa) + 30.6$ ).

### Prokaryotic determinations (abundance and biomass)

Samples for prokaryotic abundance ( $PA$ ; including bacteria, archaea and cyanobacteria) were collected into sterile Falcon vials (50 ml). Each sample was immediately fixed

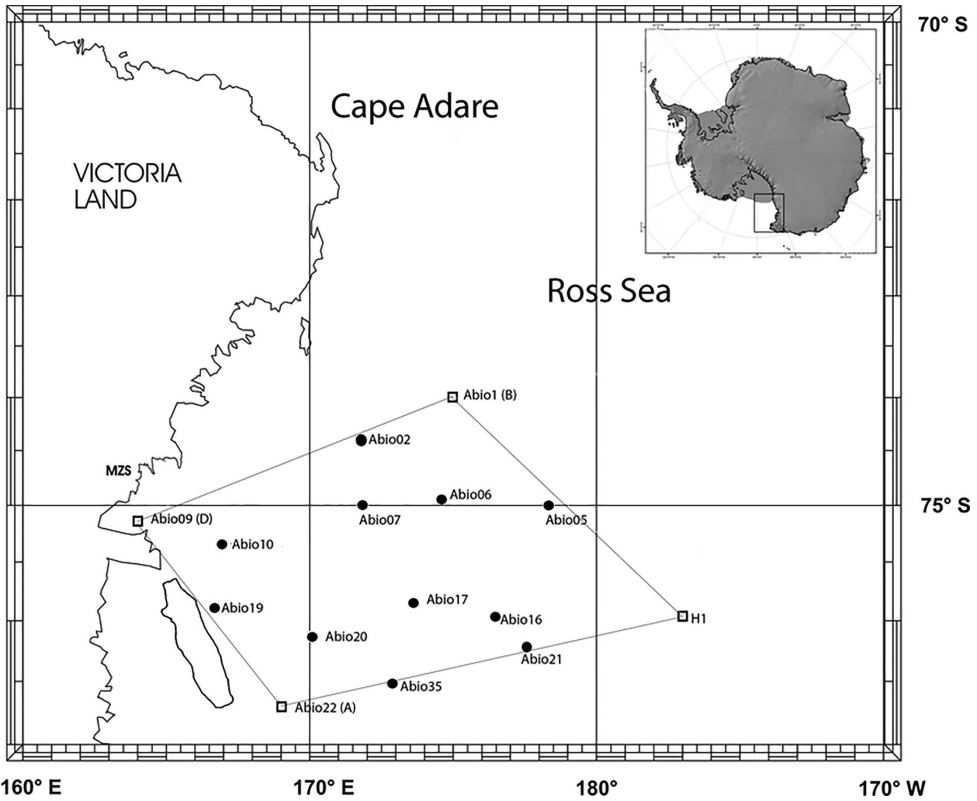


**Figure 1.** Map of the study area within the Ross Sea in the framework of the ABIOCLEAR Project in Summer 2005. The sampling stations are included within the polygon delimited by four mooring stations.

**Table 1.** Station names, sampling dates, geographical coordinates, maximum depths and basic parameters. *PA*= prokaryotic abundance; *PB*= prokaryotic biomass; *CHLa*= chlorophyll a; *ATP*= adenosine triphosphate; *ETS*= electron transport system activity; *PHA*= prokaryotic heterotrophic activity.

Station	Date	Latitude	Longitude	Depth	Studied basic parameters
Abio09-D	1/10/2005	75°06.77'S	164°25.55'E	1002	<i>PA, PB, CHLa, ATP, ETS</i>
Abio10	1/11/2005	75°20.96'S	166°54.77'E	461	<i>PA, PB, CHLa, ATP, ETS</i>
Abio19	1/16/2005	75°50.81'S	167°14.62'E	590	<i>PA, PB, CHLa, ATP, ETS</i>
Abio22-A	1/17/2005	76°41.49'S	169°04.74'E	789	<i>PA, PB, CHLa, ATP, ETS, PHA</i>
Abio01-B	1/30/2005	74°00.53'S	175°05.67'E	590	<i>PA, PB, CHLa, ATP, ETS, PHA</i>
H1	2/1/2005	75°58.20'S	177°17.64'E	616	<i>PA, PB, CHLa, ATP, ETS, PHA</i>
Abio05	2/2/2005	75°00.00'S	178°19.92'E	390	<i>PA, PB, CHLa, ATP, ETS</i>
Abio02	2/3/2005	74°17.85'S	171°35.14'E	458	<i>PA, PB, CHLa, ATP, ETS</i>
Abio06	2/4/2005	74°57.31'S	174°35.19'E	400	<i>PA, PB, CHLa, ATP, ETS, PHA</i>
Abio07	2/5/2005	75°04.92'S	171°44.70'E	548	<i>PA, PB, CHLa, ATP, ETS</i>
Abio20	2/6/2005	76°06.97'S	170°09.72'E	605	<i>PA, PB, CHLa, ATP, ETS, PHA</i>
Abio35	2/8/2005	76°30.67'S	172°17.60'E	639	<i>PA, PB, CHLa, ATP, ETS</i>
Abio21	2/8/2005	76°14.06'S	179°06.10'E	350	<i>PA, PB, CHLa, ATP, ETS</i>
Abio16	2/9/2005	75°58.39'S	176°29.49'E	454	<i>PA, PB, CHLa, ATP, ETS</i>
Abio17	2/9/2005	75°50.94'S	173°35.09'E	374	<i>PA, PB, CHLa, ATP, ETS</i>

in pre-filtered formaldehyde (0.2  $\mu\text{m}$  porosity; 2% final concentration) and stored at 4 °C until analysis. Within three months, two replicates of each sample were filtered through polycarbonate black membrane filters (0.2  $\mu\text{m}$  porosity; GE Water & Process Technologies) and stained for 10 min with 4',6-diamidino-2-phenylindole (DAPI, Sigma, final concentration 10  $\mu\text{g ml}^{-1}$ ) according to Porter and Feig (1980). Stained cells were counted under a Zeiss AXIOPLAN 2 imaging epifluorescence microscope (magnification: Plan-Neofluar 100 $\times$  objective and 10 $\times$  ocular; HBO 100 W lamp; filter sets: G365 excitation filter, FT395 chromatic beam splitter, LP420 barrier filter) equipped with the digital camera AXIOCAM-HR. Images were captured and digitised on a personal computer using the AXIOVISION 3.1 software. Linear dimensions of cells were measured and their shapes equated to standard geometric figures according to Lee and Fuhrman (1987), Fry (1990) and Massana et al. (1997). Volume of single cells (*VOL*, as  $\mu\text{m}^3$ ) was calculated according to Bratbak (1985). Cell carbon content (*CCC*, as  $\mu\text{g C cell}^{-1}$ ) was derived from cell volumes according to Loferer-Krößbacher et al. (1998). Total prokaryotic biomass (*PB*, as  $\mu\text{g C l}^{-1}$ ) was calculated by multiplying *PA* by *CCC*, locally derived from single cell *VOL* (La Ferla et al. 2015).

## Metabolic rates

### *ETS measurements and relative rates*

Respiratory rates were quantified according to the tetrazolium reduction technique (Packard 1971, 1985) as modified for the microplankton community (Kenner and Ahmed 1975). The *ETS* assay allowed an estimation of the maximum velocity (*V*<sub>max</sub>) of the dehydrogenases transferring electrons from their physiological substrates (NADH, NADPH and succinate) to a terminal electron acceptor ( $O_2$ ) through their associated electron transfer system. Details on our *ETS* measurements in Antarctic and peri-Antarctic areas have been described previously (Azzaro et al. 2006, Crisafi et al. 2010, Misic et al. 2017). Briefly, subsamples (from 2 to 20 l) were pre-filtered through a 250- $\mu\text{m}$  mesh-size net and concentrated on GF/F-glass-fibre filters (nominal pore diameter 0.7  $\mu\text{m}$ ) at reduced pressure (< 1/3 atm). Although the filter porosity was specific for microplankton, GF/F filters retain also particles colonised by very small heterotrophs. The filters were immediately folded into cryovials and stored in liquid nitrogen to prevent the enzymatic decay (Ahmed et al. 1976) until they were analysed in the laboratory (< 3 months). The assays were performed in duplicate and homogenates were incubated for 30 min in the dark at the *in situ* temperature ( $\pm 0.5$  °C) of the sample. The *ETS* was corrected for *in situ* temperature with the Arrhenius equation using a value for the activation energy of 11.0  $\text{kcal mol}^{-1}$  (Packard et al. 1975, Arístegui and Montero 1995).

The specific standard deviation (i.e. the percentage of the standard deviation of the replicates on the average value of the same replicates), due to the analytical procedures and sample handling, was about 35%.

$ETS$  ( $\mu\text{l O}_2 \text{ l}^{-1} \text{ h}^{-1}$ ) was considered equal to the respiration rate in the epipelagic zone and converted to respiratory Carbon Dioxide Production Rates ( $CDPR$ ) ( $\mu\text{g C l}^{-1} \text{ d}^{-1}$ ) by using the following (Eq.1):

$$CDPR = (ETS * 12 / 22.4) * (122 / 172) \text{ (Eq.1)}$$

where 12 is the C atomic weight, 22.4 the  $\text{O}_2$  molar volume and 172/122 the Takahashi oxygen/carbon molar ratio (Takahashi et al. 1985). Real respiratory rates have been calculated using the conversion factors from  $ETS$   $V_{\text{max}}$  to  $CDPR$  as referred by La Ferla and Azzaro (2001b) and Azzaro et al. (2006), in the epi- and mesopelagic layers, respectively.

Cell specific respiratory rates ( $CSRR$ ) were calculated by dividing normalised  $CDPR$  values to the normalised cell abundance values in each station by adopting a prokaryotic contribution of 50% and 80% at epipelagic and mesopelagic layers, respectively, assuming that the activities we measured were mainly due to the prokaryotic fraction and that all the cells have similar activity levels.

### ***Heterotrophic energy production (HEP) determination***

Today, the P/O ratio is thought to be closer to 2.5 rather than 3.0 (Ferguson 2010, Moran et al. 2012). With this ratio and using  $ETS$  activities to compute respiration, one can derive  $ATP$  production rates in a particular oceanic region through the determination of the  $HEP$  (Packard et al. 2015).  $HEP$ , in micro Joules ( $\mu\text{J}$ ), can be calculated from seawater respiration ( $R$ ) in  $\mu\text{mol O}_2 \text{ h}^{-1} \text{ l}^{-1}$  using the following equation (Eq.2):

$$HEP (\mu\text{J h}^{-1} \text{ l}^{-1}) = R (\mu\text{mol O}_2 \text{ h}^{-1} \text{ l}^{-1}) * 2 * 2.5 * 0.048 * 10^{-6} \text{ (Eq.2)}$$

where 2 is the number of electron pairs that participate in reduction of one molecule of  $\text{O}_2$  to two molecules of  $\text{H}_2\text{O}$ ; 2.5 is the modified P/O of Ochoa (1943), the  $ATP$  produced by the flow of one electron pair; 0.048 is the Gibbs Free Energy ( $\Delta G$ ) per micro mol  $ATP$  in  $\text{J} \cdot (\mu\text{mol } ATP)^{-1}$  (Hinkle 2005, Ferguson 2010, Moran et al. 2012, Packard et al. 2015); and  $10^{-6}$  converts Joules to micro Joules. If,  $HEP$  in milli Joules ( $\text{mJ}$ ) is desired, simply replace the factor,  $10^{-6}$ , in Eq. 2, with the factor,  $10^{-3}$ . The turnover time ( $\tau$ ) of  $ATP$  in the microplankton community, from which came the sample, is the molar ratio of the  $ATP$  concentration to the  $ATP$  production rate, in the microplankton. The calculation steps are shown in Table 2.

### ***Prokaryotic heterotrophic activity (PHA) and production (PHP)***

$PHA$  was evaluated by  $^3\text{H}$ -leucine incorporation rate assay using the microtubes method described by Smith and Azam (1992). Briefly, triplicate 1.7 ml subsamples and duplicate zero-time killed (trichloroacetic acid-TCA, 5% final concentration) blanks were

**Table 2.** Heterotrophic Energy production (*HEP*) and adenosine triphosphate (*ATP*) turnover time in microplankton in the Ross Sea water column.

Pelagic Zone	Depth Interval (m)	Potential Respiration ( $\Phi$ ) ( $\mu\text{mol O}_2 \text{ l}^{-1} \text{ h}^{-1}$ )	<i>ATP</i> ( $\text{ng l}^{-1}$ )	Respiration ( $\mu\text{mol O}_2 \text{ l}^{-1} \text{ h}^{-1}$ )	<i>HEP</i> ( <i>ATP</i> Production) ( $\mu\text{mol l}^{-1} \text{ h}^{-1}$ )	<i>HEP</i> (Energy Production) ( $\text{mJ l}^{-1} \text{ h}^{-1}$ )	<i>ATP</i> Turnover Time ( $\tau$ ) (min)
Euphotic	2–100	9.13 $\pm$ 5.93	123 $\pm$ 72.2	2.38 $\pm$ 1.54	11.88 $\pm$ 7.71	570 $\pm$ 370	1.25 $\pm$ 0.76
Epipelagic	2–160	8.97 $\pm$ 3.27	110 $\pm$ 71.0	2.33 $\pm$ 0.85	11.67 $\pm$ 4.25	560 $\pm$ 204	1.15 $\pm$ 0.77
Mesopelagic Upper (A)	100–500	4.02 $\pm$ 3.49	30.35 $\pm$ 31.68	1.05 $\pm$ 0.91	5.23 $\pm$ 4.54	251 $\pm$ 218	0.74 $\pm$ 0.49
Mesopelagic Upper (B)	160–500	3.03 $\pm$ 3.19	27.49 $\pm$ 32.58	0.86 $\pm$ 0.83	4.31 $\pm$ 4.15	207 $\pm$ 199	0.78 $\pm$ 0.53
Mesopelagic lower	500–800	1.65 $\pm$ 0.88	13.48 $\pm$ 6.76	0.43 $\pm$ 0.23	2.15 $\pm$ 1.15	103 $\pm$ 55	0.76 $\pm$ 0.53

incubated in 2 ml polypropylene microcentrifuge tubes (Safe-lock, Eppendorf) with L-[4,5- $^3\text{H}$ ] leucine (Amersham, GE Healthcare, SA 61Ci/mmol) giving final concentration of 20 nM. Microtubes were distributed in floating racks into darkened containers with seawater disposed in a refrigerated box. Samples were incubated for 170–190 min at a temperature between  $-0.5$  and  $-0.8$   $^{\circ}\text{C}$ . Incubation was stopped with TCA (5% final concentration). Pellets were washed twice with 5% TCA and 80% ethanol and finally supplemented with 1 ml of liquid scintillation cocktail (Ultima Gold MV Perkin Elmer Life and Analytical Sciences). The liquid-scintillation analysis was effected in a Perkin Elmer Model Wallac 1414 WIN Spectral counter using the internal quenching control. Saturation curves analysis and time-course experiments were carried out at four different stations (from 2 to 300 m depth) with hourly controls for up to six hours of incubation. This procedure was established in a previous cruise in the RS, carried out within the framework of the Victoria Land Transect Project – VLTP-2004 (PNRA XIX Expedition). During *PHA* time-course experiments, linearity in the  $^3\text{H}$ -leucine uptake was observed in one sample (25 m depth) between 1 and 6 hours of incubation ( $r = 0.96$ ), while in the other three samples (2, 270 and 310 m depths), linearity was observed only between 1 and 3 hours of incubation ( $r = 0.83$  and  $0.88$ , respectively).

Prokaryotic heterotrophic production (*PHP*) was calculated from the  $^3\text{H}$ -leucine incorporation rate (*PHA*) expressed in moles incorporated per unit time and volume (Kirchman et al. 1985) according to the equation  $PHP = PHA * CF$  where *CF* is a conversion factor expressed in  $\text{kg C mol}^{-1}$ . *CF* were determined following a “semi-theoretical” approach using the molecular weight of leucine, the leucine content of cellular protein and the cellular carbon equivalent of the protein according to Simon and Azam (1989) and the isotope dilution (*ID*) *in situ* experimentally determined according the rectangular hyperbola fitting method of van Looij and Riemann (1993), as described by Pedrós-Alió et al. (2002). In particular, *ID* was determined from two samples collected at 20 and 45 m depth, respectively and two at 300 m depth. It varied between 1.04 and 1.37. The mean value of 1.25 was used to calculate the *CF* that was equivalent to  $1.94 \text{ kg C (mol leucine)}^{-1}$  (Table 3).

*PHP* was expressed as production of biomass (as C) per time unit and volume.

**Table 3.** Isotopic Dilution (*ID*) detected from leucine incorporation rates (*V*<sub>max</sub>) in samples Abio19 (45 and 300 m depth) and Abio05 (20 and 300 m depth), respectively. *ID* mean value  $1.25 \pm 0.14$ .

Station	depth (m)	<i>V</i> <sub>max</sub> ± SD p mol l <sup>-1</sup> h <sup>-1</sup>	<i>ID</i>	confidence interval 95%
Abio19	45	18.058 ± 0.870	1.06	0.95–1.18
	300	0.357 ± 0.069	1.24	1.00–1.48
Abio05	20	9.785 ± 4.813	1.37	0.69–2.04
	300	0.932 ± 0.225	1.34	1.01–1.66

Derived parameters as Specific Growth Rate d<sup>-1</sup> [*SGR* ( $\mu$ ) = *PHP*/*PB* (Prokaryotic biomass)] and Biomass Turnover Time (days) [*BTT*(g) = ln(2)/ $\mu$ ] were calculated according to Kirchman (2001).

In comparison, *PHP*<sub>*D*</sub>, *PB*<sub>*D*</sub>, *SGR*<sub>*D*</sub> and *BTT*<sub>*D*</sub> were calculated using 107 fg C  $\mu\text{m}^{-3}$  cell and an *ID* = 1 according to Ducklow et al. (2001). Cell specific incorporation rates (*CSIR*) were calculated by dividing normalised *PHP* values to the normalised cell abundance values in each station.

The prokaryotic C requirement was computed as Prokaryotic Carbon Demand (*PCD*), i.e. *PHP*+*CDPR* by using normalised data, assuming the contribution of prokaryotes to total microbial community respiration as 50% in the epipelagic layer and a contribution of 80% in the mesopelagic ones (La Ferla et al. 2005, del Giorgio et al. 2011, Baltar et al. 2015). The Prokaryotic Growth Efficiency (*PGE*) was calculated as *PHP*/*PCD* and the isotope dilution (*ID*) *in situ* was experimentally determined according the rectangular hyperbola fitting method of van Looij and Riemann (1993), as described by Pedrós-Alió et al. (2002) using HYPER 32 fitting software.

## Data processing

In order to detect possible influences between environmental factors and microbial variables, Spearman Rank correlation coefficients were calculated for the microbiological data and environmental parameters using the SigmaStat software V3.0 and the Mann and Whitney test using the PAST.exe (Hammer et al. 2001). The analyses of variance (one-way ANOVA and Kruskal-Wallis) were applied to some parameters to assess the significance of the differences between depth layers and stations.

Data were integrated with depth according to the trapezoidal method and normalised to the depth: from 2 to 100 m for the epipelagic layer; from 100 to 800 m for the mesopelagic layer.

The depth-integrated rate ( $\int R dz$  in mg C m<sup>2</sup> d<sup>-1</sup> l<sup>-1</sup>) for the water column was calculated within the depth interval between *Z*<sub>1</sub> and *Z*<sub>2</sub> using the following equation (Eq. 3):

$$\int R dz = y (Z_2^{(x+1)} - Z_1^{(x+1)} / (x+1) \text{ (Eq.3)}$$

## Results

Temperature ranged between  $-2.01$  (H1, 500 m) and  $1.48$  °C (Abio09-D, 5 m) and salinity between  $34.11$  (Abio10, 25 m) and  $34.79$  (Abio09-D, 600 m). In Suppl. material 1: Figure S1, the temperature and salinity at surface and 200 m depth layers are shown. In the surface layer, a frontal structure was evidenced by temperature ( $T$ ) and salinity gradients. Temperature clearly decreased eastwards from  $1.5$  to  $-0.6$  °C, corresponding to mooring stations Abio09-D and H1, respectively. Salinity was similarly distributed along a non-linear front that cut eastwards and southwards through the RS with a salinity of  $34.3$ . At the 200 m depth-horizon, temperature showed a wedge of relatively warm water, with temperatures ranging from  $-1.3$  to  $-0.7$  °C, that had crept between two cooler water masses, with temperatures ranging from  $-1.9$  to  $-1.3$  °C. Salinity, in Suppl. material 1: Figure S1, showed an eastwards decreasing trend (from  $34.66$  to  $34.46$ ).

In Table 4, the ranges, mean values and standard deviations of the trophic analyses, prokaryotic determinations and metabolic rates detected in the epipelagic and mesopelagic layers are reported. *CHLa* showed very low concentrations throughout the study area (mean values  $0.14$  and  $0.058$  mg m<sup>-3</sup> in the epi- and mesopelagic layers, respectively). In the epipelagic layer, the minimum and maximum values were detected at stations Abio20 (5 m) and Abio09-D (5 m), respectively; in the mesopelagic layer, they occurred at stations Abio10 (150 m) and Abio02 (110 m), respectively.

The average *CHLa* value in the epipelagic layer was 2.4 times higher than in the mesopelagic one. In Figure 2a, the *C-CHLa* vertical distribution is reported. TSI were always lower than 30, categorising the RS as oligotrophic for Summer 2005 (Suppl. material 3: Table S2).

*ATP* sharply decreased with depth (Figure 2b) by a factor of 4 (Table 4). On average, *ATP* ranged between  $124$  and  $29$  ng l<sup>-1</sup> in the epi- and mesopelagic layers. The minimum and maximum concentrations in the epipelagic layer were observed in stations H1 (100 m) and Abio09-D (5 m), respectively; in the mesopelagic layer, at stations H1 (500 m) and Abio02 (110 m), respectively. The biological carbon, calculated from the *ATP* (*C-ATP*), decreased with depth from a mean of  $31$  micro g C l<sup>-1</sup> in the epipelagic euphotic zone to a mean of  $7$  micro g C l<sup>-1</sup> in the mesopelagic zone between 100 and 800 m (Table 4 and Figure 2b). According to Karl's classification, stations H1, Abio09-D, Abio06, Abio05 and Abio02 manifested moderate trophism ( $> 100 < 500$  ng l<sup>-1</sup>) whereas Abio07, Abio20, Abio35 manifested oligotrophy ( $ATP < 100$  ng l<sup>-1</sup>).

The calculation of the average *TSI*, chosen to establish the station trophic state, ranged from a high of 24 at H1, the most offshore station, to a low of 16 at Abio20, a station much closer to shore (Suppl. material 3: Table S2, Figure 1). Stations H1, Abio09-D, Abio21, and Abio05 were richer than the other stations. Their averaged *TSI* surpassed 23. Stations H1, Abio21 and Abio05 grouped together as the three most offshore stations, but station Abio09-D was the most inshore one. At the other end of the scale, station Abio20, as mentioned above, had the lowest *TSI*. A one-way ANOVA analysis confirmed this variability amongst the stations ( $P < 0.000314$ ,  $n = 80$ ).

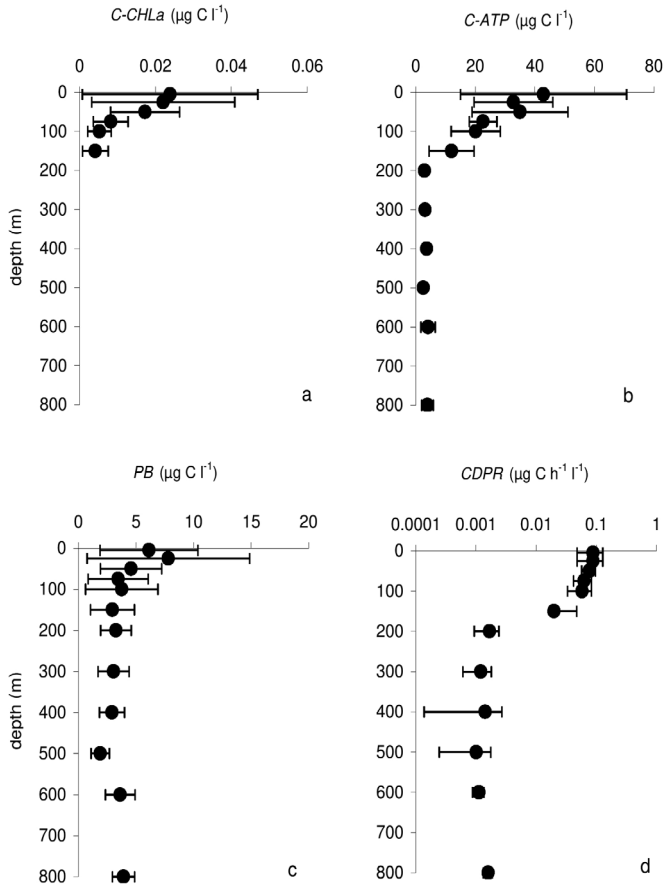


**Figure 2.** Depth profiles of mean values and standard deviations of the carbon content derived from chlorophyll *a* (*C-CHLa*, **a**) and adenosine triphosphate (*C-ATP*, **b**), the prokaryotic biomass (*PB*, **c**) and the carbon dioxide production rates derived from ETS activity (*C DPR*, **d**) in the Ross Sea water column.

Prokaryote Abundance (*PA*) was in the order of  $10^4$ – $10^6$  cell  $\text{ml}^{-1}$  in the epipelagic layer and  $10^4$ – $10^5$  cell  $\text{ml}^{-1}$  in the mesopelagic layer (Table 4). The Cell Carbon Content (*CCC*) showed a discrete variability in both the studied layers and ranged between 11 and 36 and between 13 and 45  $\text{fg C cell}^{-1}$  in epi- and mesopelagic layers, respectively (Suppl. material 4: Table S3). *PB* modulated by both *PA* and *CCC*, showed a decreasing trend and high variability in the upper layers, particularly at 25 m (Figure 2c). The minimum value was detected at 500 m and an increase below occurred. The values in the epipelagic layer were 1.7 times higher than in the mesopelagic one. In the near-surface layer, *PB* min and max values were detected at stations Abio05 (100 m) and Abio09-D (25 m), respectively. In the deep layer, *PB* min and max values were obtained at stations Abio05 (100 m) and Abio22-A (100 m), respectively.

**Table 4.** Range, mean and standard deviations, sampling numbers (n) of trophic parameters (*CHLa*, *C-CHLa*, *ATP* and *C-ATP*), prokaryotic abundance and biomass (*PA* and *PB*) and metabolic rates (*ETS*, *CDPR* and *PHP*); detected in the epipelagic (0–100 m) and mesopelagic (>100<800 m) depth layers. *CHLa*= chlorophyll *a*; *C-CHLa*= chlorophyll *a* in carbon units; *ATP*= adenosine triphosphate; *C-ATP*= adenosine triphosphate in carbon units; *PA*= prokaryotic abundance; *PB*= prokaryotic biomass; *ETS*= electron transport system activity; *CDPR*= carbon dioxide production rate; *PHP*= carbon prokaryotic heterotrophic production.

	<i>CHLa</i> mg m <sup>-3</sup>	<i>C-CHLa</i> mg C m <sup>-3</sup>	<i>ATP</i> ng l <sup>-1</sup>	<i>C-ATP</i> ng C l <sup>-1</sup>	<i>PA</i> cells ml <sup>-1</sup>	<i>PB</i> µg C l <sup>-1</sup>	<i>ETS</i> µl O <sub>2</sub> l <sup>-1</sup> h <sup>-1</sup>	<i>CDPR</i> µg C l <sup>-1</sup> h <sup>-1</sup>	<i>PHP</i> µg C l <sup>-1</sup> h <sup>-1</sup>
0–100 m depth									
min	0.019	1.89	42.76	10689	5.70E+4	0.8	0.052	0.0043	0.0005
max	0.539	53.90	380.49	95123	1.44E+6	24.5	0.437	0.1660	0.0295
mean	0.141	14.11	123.78	30944	2.87E+5	5.2	0.201	0.0740	0.0100
SD	0.116	11.56	70.26	17564	2.55E+5	4.5	0.076	0.0323	0.0077
n	67	67	39	39	67	67	66	66	25
100–800 m depth									
min	0.007	0.67	4.77	1193	5.66E+4	0.8	0.006	0.0002	0.0003
max	0.244	24.44	130.69	32673	6.76E+5	15.1	0.271	0.0965	0.0061
mean	0.058	5.77	29.04	7260	1.51E+5	3.1	0.086	0.0122	0.0019
SD	0.051	5.14	30.66	7664	8.45E+4	1.9	0.076	0.0244	0.0015
n	25	25	47	47	78	78	81	81	36

*ETS* showed a decreasing trend with depth and the values in the epipelagic layer were 3 times higher than in the mesopelagic one (Table 4). In the upper layer, *ETS* minimum and maximum values were detected at stations Abio 22-A (80 m) and Abio10 (25 m), respectively. In the deeper layer, they were observed at stations Abio16 (400 m) and Abio10 (150 m), respectively.

*CDPR* showed a decreasing trend with depth with a discrete variability in the deep layers (Figure 2d). It sharply decreased with depth by a factor of 6 (Table 4). The minimum value in the epipelagic layer was achieved at station Abio16 (2 m) and the maximum value at Abio10 (25 m). In the mesopelagic layer, minimum and maximum values were observed at Abio16 (400 m) and Abio17 (120 m), respectively.

The cell specific respiratory rate (*CSRR*) calculated on depth-integrated and normalised data (Figure 3), in the epipelagic layer varied between  $10.1 \times 10^{-3}$  (Abio16) and  $390 \times 10^{-3}$  (at station Abio02) fg C cell<sup>-1</sup>; in the mesopelagic waters, they varied between  $1.46 \times 10^{-3}$  (Abio16) and  $50.1 \times 10^{-3}$  (Abio17) fg C cell<sup>-1</sup>.

The *HEP* calculations for the epipelagic and mesopelagic waters of RS are given in Table 2. The average *HEP* (and standard deviation) in epipelagic zone down to 160 m was  $560 \pm 20 \mu\text{J h}^{-1} \text{l}^{-1}$ . Over this depth range, *HEP* ranged from as high of  $108 \mu\text{J h}^{-1} \text{l}^{-1}$ , at station Abio06 (2 m depth), to  $15 \mu\text{J h}^{-1} \text{l}^{-1}$ , at station Abio22-A (80 m). The *HEP* calculations for the euphotic zone (upper 100 m) were the same (Line 1, Table 2). The range was 108 to  $15 \mu\text{J h}^{-1} \text{l}^{-1}$  and the average and standard deviation was  $570 \pm 370 \mu\text{J h}^{-1} \text{l}^{-1}$ . In mesopelagic waters below 160 m down to 500 m, *HEP* was 80% lower, averaging  $118 \pm 90 \mu\text{J h}^{-1} \text{l}^{-1}$ . If we make the calculation from and including 100, the *HEP* down to 500 m was larger. It averaged  $251 \pm 218 \mu\text{J h}^{-1} \text{l}^{-1}$ . The database for

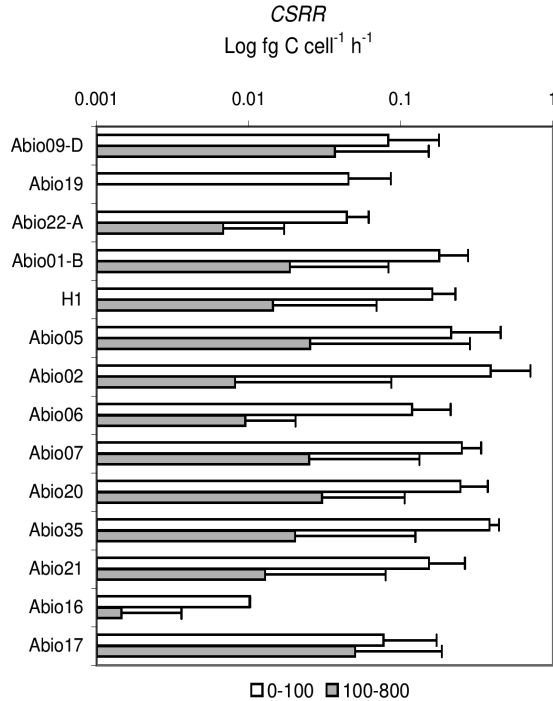


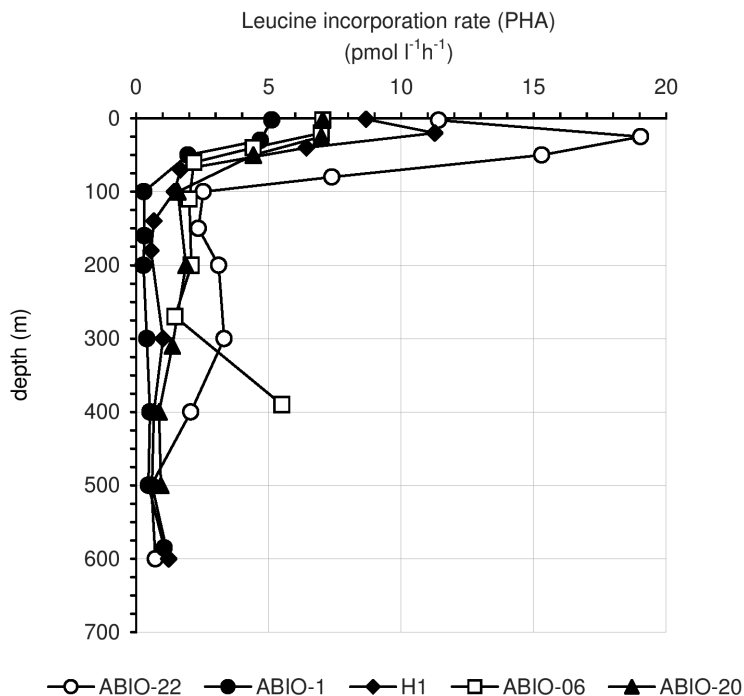
**Figure 3.** Cell Specific Respiratory Rates (*CSRR*) and SD for each station in the epipelagic and mesopelagic layers (0–100 m, 100–800 m). In the upper and deeper layers, the prokaryotic contributions to total respiration were considered to be the 50% and 80%, respectively, of the total carbon dioxide production rates (*CDPR*).

the mesopelagic waters between 500 and 800 m was smaller than the one between 100 and 500 m, in only 15 compared to 74 measurements. These measurements yielded an average deep-mesopelagic *HEP* of  $103 \pm 55 \mu\text{J h}^{-1} \text{l}^{-1}$ . The *ATP* turnover rate in the cells of the microplankton was remarkably constant with depth, in the order of magnitude of a minute. It only decreased 39% from the euphotic zone to the lower mesopelagic zone, from  $1.25 \pm 0.76$  to  $0.76 \pm 0.53$  minutes.

The prokaryotic heterotrophic activity (*PHA*) – in term of leucine incorporation rates – varied between 0.213 and 19.035  $\text{pmol l}^{-1} \text{h}^{-1}$  (Figure 4). Peaks of activity were detected in surface (Abio01-B, Abio20 and Abio06 stations) or at 20–25 m depth (Abio22-A and H1 stations). Decreasing *PHA* was detected with depth followed by an increase of activity in the bottom samples (Figure 4). In station Abio22-A, normalised *PHA* in the epipelagic layer ( $12.4 \text{ nmol m}^{-3} \text{h}^{-1}$ ) was one order of magnitude higher than that observed in the other stations (Table 5). *PHA* observed in 0–50 m layers was on average  $8.05 \pm 4.52 \text{ pmol l}^{-1} \text{h}^{-1}$  ( $n = 15$ ). The cell specific incorporation rate (*CSIR*) varied between 1.992 and 70.844  $\text{z mol leucine cell}^{-1} \text{h}^{-1}$  with the highest values in the upper 50 m depth ( $28.20 \pm 15.97 \text{ z mol leucine cell}^{-1} \text{h}^{-1}$ ) while, in mesopelagic waters, they turned out to be one order of magnitude less ( $6.48 \pm 3.63 \text{ z mol leucine cell}^{-1} \text{h}^{-1}$ ,  $n = 26$ ). Throughout the different water columns, *CSIR* strictly reflected what has already been observed in *PHA* (see Figure 4).

**Table 5.** Leucine incorporation rates (*PHA* expressed in  $\text{nmol m}^{-3} \text{h}^{-1}$ ) integrated in the depth intervals 1–100 m (epipelagic layer) and 100 m–bottom (mesopelagic layer) and normalized.

Station	depth (m)	<i>PHA</i>	
		1–100 m	100 m – bottom (m)
Abio22-A	789	12.420	2.093 (600)
Abio01-B	590	2.651	0.463 (585)
H1	616	5.398	0.799 (600)
Abio06	400	3.805	2.589 (390)
Abio20	605	3.926	1.353 (500)

**Figure 4.** Leucine incorporation rates (*PHA*) at the five stations in the Ross Sea, Summer 2005.

*PHP* showed the same distribution of *PHA* throughout the water column. In the epipelagic layer, *PHP* varied between 0.46 and 29.51  $\text{ng C l}^{-1} \text{h}^{-1}$  with the highest value at station Abio22-A at 25 m depth. In mesopelagic waters, *PHP* varied 0.33 and 6.11  $\text{ng C l}^{-1} \text{h}^{-1}$  and it was, on average, 5 times lower than in upper layer (Table 4). In Table 6, the *PHP*, *PB*, *SGR* and *BTT* calculated at the ABIO22, ABIO01, H1, ABIO06 and ABIO20 stations are reported. In the euphotic layer, *SGR*  $\text{day}^{-1}$  ranged from 0.005 to 0.18 with a mean of 0.053. With the conversion factors used by Ducklow et al. (2001), *SGR<sub>D</sub>*  $\text{day}^{-1}$  ranged from 0.013 to 0.44, with a mean of 0.128. Contrary to the *SGR*, the *BTT* (days) ranged from 3.79 to 128.31 (mean = 28.1) and *BTT<sub>D</sub>* ranged from 1.55 to 52.04 (mean = 11.6). In mesopelagic waters, *SGR* and *BTT* were lower and higher, respectively, than those observed in the upper 100 m of the epipelagic zone.

**Table 6.** Prokaryotic heterotrophic production (*PHP*), Prokaryotic biomass (*PB*), Prokaryotic specific growth rate (*SGR*) and Biomass turnover time (*BTT*) calculated in the five indagated stations (ABIO22, ABIO01, H1, ABIO06 and ABIO20).  $PHP_D$ ,  $PB_D$ ,  $SGR_D$  and  $BTT_D$  were calculated using a different factor ( $107 \text{ fg C } \mu\text{m}^{-3} \text{ cell}^{-1}$  and  $ID = 1$ ) according to Ducklow et al. (2001).

	Depth	n	Mean	SD	Range
<i>PHP</i> ( $\text{ng C l}^{-1} \text{ h}^{-1}$ )	0–100 m	22	12.182	9.492	0.575–36.883
	100–800 m	26	2.027	1.629	0.413–6.441
$PHP_D$ ( $\text{ng C l}^{-1} \text{ h}^{-1}$ )	0–100 m	22	9.746	7.593	0.460–29.506
	100–800 m	26	1.622	1.303	0.330–5.153
<i>PB</i> ( $\mu\text{g C l}^{-1}$ )	0–100 m	20	5.179	3.594	1.921–15.127
	100–800 m	25	3.222	1.939	1.074–9.028
$PB_D$ ( $\mu\text{g C l}^{-1}$ )	0–100 m	20	1.735	1.242	0.608–5.125
	100–800 m	25	1.077	0.676	0.338–3.101
<i>SGR</i> $\text{day}^{-1}$	0–100 m	20	0.053	0.047	0.005–0.183
	100–800 m	25	0.016	0.011	0.003–0.038
$SGR_D$ $\text{day}^{-1}$	0–100 m	20	0.128	0.116	0.013–0.446
	100–800 m	25	0.040	0.027	0.006–0.095
<i>BTT</i> (days)	0–100 m	20	28.12	30.43	3.79–128.31
	100–800 m	25	65.29	50.44	18.24–254.05
$BTT_D$ (days)	0–100 m	20	11.63	12.50	1.55–52.04
	100–800 m	25	27.458	23.152	7.26–118.26

**Table 7.** Prokaryotic carbon demand (*PCD*) and prokaryotic growth efficiency (*PGE*) depth-integrated and normalized values in the epi- and mesopelagic depth layers.

Station	0–100 m depth		100–800 m depth	
	<i>PCD</i>	<i>PGE</i>	<i>PCD</i>	<i>PGE</i>
	$\text{mg C m}^{-3} \text{ h}^{-1}$	%	$\text{mg C m}^{-3} \text{ h}^{-1}$	%
Abio09-D	–	–	0.0069	26.23
Abio22-A	0.051	37.82	0.0052	60.21
Abio01-B	0.0354	11.62	0.0052	22.28
H1	0.0417	19.87	0.0045	27.58
Abio06	0.0551	18.99	0.0029	26.21
Abio20	0.0457	13.31	0.0079	26.71
Abio16	–	–	0.0037	88.49

The normalised prokaryotic C demand (*PCD*) ranged between 0.035 and 0.055  $\text{mg C h}^{-1} \text{ m}^{-3}$  in the epipelagic layer with high values at Abio22-A and Abio06. In the mesopelagic layer, it ranged between 0.003 and 0.008  $\text{mg C h}^{-1} \text{ m}^{-3}$  with the highest value at Abio20 (Table 7). Comparing the two layers, the averaged *PCD* was about 9 times higher in the epipelagic layer than in mesopelagic one (Kruskal-Wallis One-Way ANOVA:  $P < 0.003$ ).

The normalised *PGE* ranged between 12 and 37% in epipelagic layer, with the lowest value at Abio01-B and the highest at Abio22-A. In the mesopelagic layer, *PGE* ranged between 22 and 88% with the minimum value at station Abio01-B and the maximum at Abio16. In contrast to the *PCD*, the averaged *PGE* was twice as high in the mesopelagic zone as in the epipelagic one (Kruskal-Wallis One-Way ANOVA:  $P < 0.048$ ).

**Table 8.** Spearman–Rank correlations among microbial and environmental parameters in the whole data set.  $O_2$ = dissolved oxygen; S= salinity; DEN= density; PA= prokaryotic abundance; PB= prokaryotic biomass; CCC= cell carbon content; ATP= adenosine triphosphate; CHLa= chorophyll a; PHP= prokaryotic heterotrophic production; CDPR= carbon dioxide production rates.

<i>CHLa vs.</i>	<i>r</i>	<i>P</i>	<i>n</i>	<i>ATP vs.</i>	<i>r</i>	<i>P</i>	<i>n</i>
Depth	-0.545	0.0000	80	Depth	-0.836	0.0000	79
<i>T</i> °C	0.5	0.0000	80	<i>T</i> °C	0.776	0.0000	78
$O_2$	0.626	0.0000	73	$O_2$	0.543	0.0000	67
S	-0.505	0.0000	73	S	-0.762	0.0000	67
DEN	-0.522	0.0000	73	DEN	-0.747	0.0000	67
PA	0.347	0.0024	75	PA	0.399	0.0000	78
PB	0.318	0.0056	75	CCC	-0.255	0.0243	78
ATP	0.899	0.0000	42	PB	0.229	0.0437	78
PHP	0.46	0.0139	28	CHLa	0.899	0.0000	42
CDPR	0.346	0.0028	73	CDPR	0.775	0.0000	76

<i>PB vs.</i>	<i>r</i>	<i>P</i>	<i>n</i>	<i>CDPR vs.</i>	<i>r</i>	<i>P</i>	<i>n</i>	<i>PHP vs.</i>	<i>r</i>	<i>P</i>	<i>n</i>
Depth	-0.285	0.0000	134	Depth	-0.851	0.0000	136	Depth	-0.683	0.0000	56
<i>T</i> °C	0.197	0.023	134	<i>T</i> °C	0.714	0.0000	136	<i>T</i> °C	0.47	0.0000	56
$O_2$	0.459	0.0000	122	$O_2$	0.607	0.0000	123	$O_2$	0.784	0.0000	47
S	-0.215	0.0174	122	S	-0.731	0.0000	123	S	-0.545	0.0000	47
DEN	-0.205	0.0237	122	DEN	-0.726	0.0000	123	DEN	-0.554	0.0000	47
PA	0.898	0.0000	134	PA	0.304	0.0000	125	PA	0.662	0.0000	56
CCC	0.258	0.0027	134	CCC	-0.256	0.0040	125	PB	0.618	0.0000	56
ATP	0.229	0.0437	78	PB	0.216	0.0157	125	CHLa	0.46	0.0139	28
CHLa	0.318	0.0056	75	CHLa	0.346	0.0028	73	ETS	0.615	0.0000	54
PHP	0.618	0.0000	56	ATP	0.775	0.0000	76	CDPR	0.657	0.0000	54
CDPR	0.216	0.0157	125	PHP	0.657	0.0000	54				

The Spearman–Rank correlation analysis of the whole dataset yielded the outputs shown in Table 8; only the significant correlation coefficients (*r*) are reported, together with their significance level (*P*) and data number (*n*). Numerous significant correlations were computed amongst the hydrological, trophic and microbial parameters. PB, CDPR and PHP showed the largest number of highly significant correlations with most of the hydrological, trophic and microbiological parameters. No significant relations were detected between CCC vs. PHP and CHL or between PHP and ATP. In Table 9, the stations and depths, which showed the minimum and maximum values of each parameter in the epi- and mesopelagic layers, are summarised. Finally, the depth integrated data of standing stock - in terms of prokaryotic and autotrophic biomass (PB and C-CHLa), total biomass (C-ATP) and remaining heterotrophic biomass (HB) – and rates – in terms of respiratory and prokaryotic heterotrophic production rates (CDPR and PHP) – are reported in Suppl material 5: Table S4, C-CHLa, PB and C-ATP, amounted to 1545, 1681 and 4605 mg C m<sup>-2</sup>, respectively. The remaining heterotrophic component (HB) presumably accounted for a biomass of 1379 mg C m<sup>-2</sup>. CDPR remineralised 8.279 mg C m<sup>-2</sup> h<sup>-1</sup> with higher rates in the upper layers while PHP accounted for 1.697 mg C m<sup>-2</sup> h<sup>-1</sup> with a similar weight in the epi- and mesopelagic layers.

**Table 9.** Stations and depth with minimum and maximum values of each parameters in the epi- and meso-pelagic layers. *CHLa*= chlorophyll *a*; *ATP*= adenosine triphosphate; *PA*= prokaryotic abundance; *CCC*= cell carbon content; *PB*= prokaryotic biomass; *ETS*= electron transport system activity; *CDPR*= carbon dioxide production rates; *PHA*= prokaryotic heterotrophic activity.

	0–100 m		100–800 m	
	min	max	min	max
<i>CHLa</i>	Abio20 – 5m	Abio09(D) – 5m	Abio10 – 150m	Abio02 – 110m
<i>ATP</i>	H1 – 100m	Abio09(D) – 5m	H1 – 500m	Abio02 – 110m
<i>PA</i>	Abio05 – 100m	Abio09(D) – 25m	Abio22(A) – 100m	Abio07 – 500m
<i>CCC</i>	Abio20 – 2m	H1 – 2m	Abio05 – 200m	Abio09(D) – 800m
<i>PB</i>	Abio05 – 100m	Abio09(D) – 25m	Abio05 – 100m	Abio22(A) – 100m
<i>ETS</i>	Abio22(A) – 80m	Abio10 – 25m	Abio16 – 400m	Abio10 – 150m
<i>CDPR</i>	Abio16 – 2m	Abio10 – 25m	Abio16 – 400m	Abio17 – 120m
<i>HEP</i>	Abio22(A) – 80m	Abio06 – 2m	Abio16 – 400m	Abio10 – 150m
<i>PHA</i>	Abio01(B) – 100m	Abio22(A) – 25m	Abio06 – 270m	Abio16 – 250m

## Discussion

### Trophic conditions and prokaryotic biomass

The environmental assessment revealed a general picture of low trophism on a spatial scale as exemplified by the *CHLa* concentration. Analysis of the *ATP* concentrations also indicated modest or poor trophism. Considering *ATP* as a quantitative proxy for total living biomass (Holm-Hansen and Paerl 1972, Karl 1980), a relatively homogeneous biomass occurred throughout the RS. However, according to Karl's classification, most stations manifested moderate trophism or oligotrophy. In a previous study carried out in January-February 2001 in the RS, an extensive algal biomass and variable *ATP* estimates corresponding to different trophic statuses were observed (Azzaro et al. 2006, La Ferla et al. 2015). In particular, marked peaks of *ATP* were found (up to 1752 ng l<sup>-1</sup>), revealing strong eutrophy according to Karl (1980). In our study, *ATP* determinations confirmed the trophic evaluation derived by *TSI*. In the 0–100 m depth layer, the autotrophic biomass (in terms of *C-CHLa*) accounted for 20–59% (mean value 44 ± 19%) of the total biomass (in terms of *C-ATP*). The highest and the lowest ratios of autotrophic biomass occurred at stations Abio09-D and Abio20, respectively, thus corroborating the previous statements about *TSI* and *ATP* estimates. In the epipelagic layer, the integrated *CHLa* values revealed a low phytoplankton standing stock varying from 4.76 to 23.68 mg m<sup>-2</sup>. In contrast, in austral summer 2014, Mangoni et al. (2017) detected high autotrophic biomass (integrated *CHLa* up to 371 mg m<sup>-2</sup>) in the epipelagic layer of the RS.

*PA* was in a range comparable to similar measurements made in several Antarctic marine environments (see table S1 in La Ferla et al. 2015). Comparison to previous studies in the RS confirmed the results of Monticelli et al. (2003) in Terra Nova Bay and Celussi et al. (2009) in Cape Adare.

*PB* decreased with depth by a factor of 1.7. However, it was higher than other prokaryotic measurements made previously in the RS (Buitenhuis et al. 2012, Carlson et al. 1999, Steward and Fritsen 2004). The utilisation of a variable cell carbon content (from 11 to 45) to calculate the biomass in each sample could partially explain this pattern. Generally, two standard PA to biomass conversion factors are utilised in ecological marine studies: 20 fg C cell<sup>-1</sup> (Lee and Fuhrman 1987) or 9.1 fg C cell<sup>-1</sup> (Buitenhuis et al. 2012). Since cell carbon content is directly linked to cell-size variability (Young 2006), the utilisation of unvarying factors to convert abundance to biomass might distort the evaluations by overestimating or, in this case, underestimating the actual carbon amounts (La Ferla et al. 2015).

### Respiration and CO<sub>2</sub> production

The *ETS* assay, originally designed by Packard (1971), continues to be successfully adopted in oceanic regions because of its high sensitivity and resolution levels that are not attainable with other methods based on sample incubation (del Giorgio and Williams 2005). Moreover, the response to the bias derived by the utilisation of empirical conversion factors from the *ETS* *V*<sub>max</sub> into actual rates of O<sub>2</sub> consumption and metabolic CO<sub>2</sub> production has largely been discussed and countered (del Giorgio and Williams 2005, La Ferla et al. 2010, Packard et al. 2015, Filella et al. 2018). Independently, good correlations between *ETS* and *in vivo* respiration rates were obtained in surface seawater samples in the framework of the ABIOCLEAR cruise. In the aphotic zone between 100 and 600 m depth of the RS, Azzaro et al. (2006) reported decreasing *ETS* activity throughout the water column and, despite the algal bloom in 2001, the *ETS* activity fell in a narrower range (0.017–0.170 μl O<sub>2</sub> l<sup>-1</sup> h<sup>-1</sup>) than our data in the mesopelagic layer. In Summer 2014, Mistic et al. (2017) observed different *ETS* - *POM* relationships, but ones consistent with the characteristics of a phytoplanktonic bloom of the *Phaeocystis* type. Moreover, their results featured averaged *ETS* values twice ours in the epipelagic and mesopelagic layers. *CDPR* was also twice ours in the upper layers and 4.6 times higher than ours in the mesopelagic one. The comparison between these findings evidenced great differences in the metabolic rates on an inter-annual scale and corroborated the importance of heterotrophic signals in understanding climate trends.

### Heterotrophic energy production

*HEP* calculations in the microplankton quantify the energy generation due to the decomposition of *ATP* by a group of enzymes (*ATPases*) in plasmalemma membranes of constituent bacteria and archaea as well as in constituent eukaryote mitochondrion. It represents a new metric in oceanographic analysis. The only other oceanic region, for which *HEP* has been calculated, is the Peru Current Upwelling at 15° S (Pisco, Peru).

The *HEP* calculations for the epipelagic and mesopelagic waters of the Peru Upwelling at 15° S are given in Packard et al. (2015). The average *HEP* (and standard deviation) in the epipelagic zone down to 150 m was  $24 \pm 30 \times 10^3 \mu\text{J h}^{-1} \text{l}^{-1}$ . In a transect (C-Line) for 185 km across the Peru Upwelling, epipelagic *HEP* ranged from a high of  $108 \times 10^3 \mu\text{J h}^{-1} \text{l}^{-1}$ , at station C10, over the Peru Trench, 71 km from the coast, to a low of  $2 \times 10^3 \mu\text{J h}^{-1} \text{l}^{-1}$ , 22 km further offshore at station C12. In mesopelagic waters below 150 m down to 1000 m, *HEP* was 96% lower than it was in the epipelagic zone, averaging only  $84 \pm 59 \mu\text{J h}^{-1} \text{l}^{-1}$ . These values, from the Peru Upwelling system (Packard et al. 2015), are more than an order of magnitude higher than the values from the RS.

### Prokaryotic heterotrophic activity and production

Time course experiments on *PHA* showed results in agreement with those detected in the VLTP-2004 project (Monticelli, personal communication). Linearity occurred within 1 and 6 hours for samples collected at 25 m depth and in a smaller time lapse for the others. Along the water column, higher *PHA* was always observed in the photic layers while reduced activity in the aphotic waters occurred. An increase in activity was always observed in the bottom samples, i.e. those taken a few metres from the sea floor. The increase of heterotrophic bacteria metabolisms in benthic boundary layers is a known phenomenon observed in other water columns (Packard and Christensen 2004).

At station Abio22-A, *PHA* was particularly high at all depths, with the highest normalised rates ( $12.442 \text{ nmol m}^{-3} \text{ h}^{-1}$ ) in the photic layer. This was one order of magnitude higher than equivalent normalised *PHA* calculations observed at the other four stations. The mean leucine incorporation rate observed in the 0 - 50 m layer was  $8.05 \text{ pmol l}^{-1} \text{ h}^{-1}$  (sd = 4.52, n = 15), the same order of magnitude as observed by Ducklow et al. (2001) in the RS during late spring period. The *PHA* observed in our cruise was also in accordance with that observed by Pedrós-Alió et al. (2002) in the Gerlache strait (Antarctic Peninsula) in late spring and summer cruises. The cell specific incorporation rate (*CSIR*) strictly reflected the distribution of *PHA* throughout the water column with the highest values in the surface to 50 m depth layer.

In our experiment, an isotope dilution of 1.25 was used to calculate the *CF*. It was equivalent to  $1.94 \text{ kg C mol leu}^{-1}$ . Considering the variability observed in *ID* determinations and the coefficient of variation (CV%) detected in the triplicate samples for leucine incorporation-rate analysis (mean = 14.3%, sd = 11.3%, n = 84), the *ID* should be not too far from 1 (assuming no isotope dilution). That value corresponds to a theoretical *CF* =  $1.55 \text{ kg C mol leu}^{-1}$  (Simon and Azam 1989). Similar *ID* values (mean = 1.27 corresponding to *CF* =  $1.96 \text{ kg C mol leu}^{-1}$ ) were detected in the Antarctic Peninsula area in late spring-summer where the empirical method carried out simultaneously produced on average *CF* =  $0.81 \text{ kg C mol leu}^{-1}$  (Pedrós-Alió et al. 2002). In the framework of experiments conducted in subtropical northeast Atlantic Ocean, Baltar et al. (2010) discussed the incongruence often observed between empirical and theoretical *CFs* estimates as well as their variability in the mesopelagic water column (range 0.13–

0.85 kg C mol<sup>-1</sup> leu). They argued that, in the deep domain, the carbon limitation and the slower cell growth take place, further reducing the deep water *CF*s as compared to the theoretical ones. The choice of theoretical, semi-theoretical or empirical *CF* can markedly affect the *PHP* estimation and, consequently, the derived parameters. In the case of a significantly different *CF*, it would be appropriate to use both values to furnish the best information about the carbon flux in the prokaryotic compartment. *PHP* followed the same distribution of *PHA* throughout the water column with a maximum value corresponding to a production peak at 25 m depth at station Abio22-A.

In the euphotic layer, *SGR* d<sup>-1</sup> calculated with our *CF*s, resulted 2.4 times lower than *SGR<sub>D</sub>* d<sup>-1</sup> calculated using the conversion factors used by Ducklow et al. (2001). Contrary to the *SGR*, the *BTT* (days) was 2.4 times higher than that calculated with Ducklow's *CF*s. In mesopelagic waters, *SGR* and *BTT* were the opposite of those observed in the upper 100 m of the epipelagic zone.

From mean hourly values, the *CDPR/PHP* ratios in the epi- and mesopelagic layers were 11.75 and 0.80 μg C l<sup>-1</sup> h<sup>-1</sup>, respectively.

### Prokaryotic metabolic patterns

Prokaryotic (bacterial and archaeal) activity is often measured using the *PGE* that defines the balance between catabolic and anabolic prokaryotic processes (Baltar et al. 2015). It corresponds to the proportion of dissolved organic carbon (*DOC*) that is converted by microorganisms into biomass and might be consumed by higher trophic levels (Eichinger et al. 2010). *PGE* is considered the most important factor affecting the C budget (Van Wambeke et al. 2002) and it indicates the efficiency of organic substrates recycling by prokaryotes (Mazuecos et al. 2015). The determination of *PGE* depended on the choice of the methodological procedures and approach, i.e. mostly respiration estimates and leucine to carbon *CF*. Indirect respiration estimates were often obtained from the sinking biogenic particles (Sweeney et al. 2000), from the bacterial production experimental data and from an empirical contribution of respiration (Ducklow et al. 2001; Ducklow 2003) or by sediment traps (DiTullio et al. 2000, Langone et al. 2000, Langone et al. 2003, Nelson et al. 1996). Sometimes, *PGE* is arbitrarily considered to be 30% or 36% (Manganelli et al. 2009) and a few papers have simultaneously identified the actual respiration and heterotrophic production rates (La Ferla et al. 2005, Zaccone et al. 2003, del Giorgio et al. 2011, Baltar et al. 2009, 2015 and references herein) in pelagic waters. In deep waters in the Atlantic Ocean, Baltar et al. (2010) determined *PGE* variations in the range < 1–34%. This high variability resulted in being highly correlated to the empirical conversion factors determined and adopted to calculate *PHP* (Baltar et al. 2010). High variability of *PGE*, on both space and time scales in ocean samples, has often been assessed (Lemée et al. 2002, Reinthaler and Herndl 2005) and low values of *PGE* (< 15%) have been associated with oligotrophic conditions (Biddanda et al. 2001, del Giorgio et al. 2011). In short, at low growth efficiency rates, more dissolved organic matter is remineralised,

keeping the nutrients cycling within the microbial cycle; conversely, at high growth efficiency rates, the dissolved organic matter is more efficiently transferred into the particulate phase thus strengthening the carbon distribution throughout the trophic food web (Cajal-Medrano and Maske 2005). In our study, the highest *PGE* values were determined at stations where oligotrophic conditions at the sea-surface were evidenced by *TSI*. Typically, most of the primary production in low-productivity environments is respired by bacteria (Biddanda et al. 2001). In epipelagic layers, the prokaryotic respiratory processes exceeded heterotrophic production, whilst high *PGE* was surprisingly calculated in the mesopelagic layer showing consistent differences with the upper layer. In addition, excluding the Abio16 and Abio22-A stations, where high *PHPs* were determined, the averaged *PGE* value in the mesopelagic layer surpassed the value in the epipelagic one. These findings were consistent with the high values detected in the deep layers of the Mediterranean Sea (La Ferla et al. 2005 and 2010) where *PGE* data did not correlate with primary production, but rather confirmed that the *PCD* could not be sustained solely by the *DOC* of autochthonous origin and/or by phytoplankton exudation. In the RS, Azzaro et al. (2006) compared estimates of carbon flux by sediment traps and found that about 63% of organic carbon, remineralised by respiration, was derived from the *POC* pool, confirming the decomposition rates of Ducklow et al. (2001) in the vertical *POC* flux. Weak bacteria-primary production coupling has also been ascribed to temperature restriction of metabolic utilisation (Pomeroy and Wiebe 2001) or to grazing together with the lack of bio-available dissolved organic matter (Bird and Karl 1999). The relatively high *PGE* probably also reflected the capability of prokaryotic cells to individually divide (fast growing communities) or to increase in size. We found that, in our samples, volumetric determinations in the mesopelagic layer were higher than in the epipelagic layer. They fell into the range of 0.038 to 0.196  $\mu\text{m}^3$  (data not shown). Furthermore, the circulatory dynamics of the water masses could also explain the high *PGE* at depth. When vertical convective processes occur with the sinking of surface water masses, a consequent enrichment of fresh organic matter in the deep layers happens (La Ferla and Azzaro 2001a, Azzaro et al. 2012). In temperate seas, the lateral advection of newly-formed water masses (both intermediate and deep) from convective regions as well as the lateral injection in the winter, of organic matter from the canyons and shelves, enhanced C respiration in deep layers (Packard et al. 2008, La Ferla et al. 2010). The horizontal *PGE* variability in the water layers suggested that, in mesopelagic waters, prokaryotes are able to use the available organic matter and convert it into biomass more efficiently than in epipelagic ones. This finding could be interpreted as an adaptive physiological response. It reflects the ability of deep-water microbes to efficiently exploit the available *DOC* at great depths. Placenti et al. (2018) suggested this mechanism for the deep Mediterranean Sea. Another aspect, that was unfortunately not considered, concerns the maintenance of the prokaryotic biomass and metabolism in terms of energetics when assessing the role of microbes in oceanic carbon cycles (Eichinger et al. 2010). According to Baltar et al. (2015), a combination of environmental stressors could enhance the proportion of the energy flux devoted to cell maintenance, inducing increases in cell specific respiration and decreases in *PGE*.

In incubation experiments, slow-growing bacterial communities tended to have low *PGE* and to respire a high portion of the secondary production in terms of leucine uptake (del Giorgio et al. 2011). Moreover, in oligotrophic systems, low *PGE* may result from the maintenance of active transport and from the production of exoenzymatic hydrolysis with high bacterial energy demand (del Giorgio and Cole 1998).

However, using mean hourly normalised values, the ratio *CDPR/PHP* ( $\mu\text{g C l}^{-1} \text{h}^{-1}$ ) in the epipelagic layer was 3 times higher than in the mesopelagic one, presumably due to the occurrence of autotrophic respiration (Marra and Barber 2004). The prokaryotic carbon requirement (*PCD*) was particularly low in the mesopelagic layer where autotrophic production was lacking.

The significant relationship between *CDPR* and other physical and chemical parameters measured, suggests that respiration is strictly interconnected with environmental forces. Respiration varied in response to changes in hydrology according to Rivkin and Legendre (2001). In addition, it co-varied with different microbial parameters showing the consistent patterns of diverse aspects of microbial metabolism, as previously postulated by del Giorgio et al. (2011). The close link between the diverse aspects of prokaryotic patterns would imply that changes in the metabolic variables synergistically mediate the fate of organic matter by influencing the composition of organic material reaching the sediments (Catalano et al. 2006), the distribution of particulate and dissolved matter with depth (Carlson et al. 2000, Fabiano et al. 2000, Mistic et al. 2017) and the remineralisation through the water column (Azzaro et al. 2006, 2012).

In all the stations, *CSRR* was surprisingly higher in the epipelagic layer than in the mesopelagic one. This suggests that a valuable contribution of organic matter of phytoplanktonic origin might sustain the heterotrophic metabolism in the upper layer. When we calculate *CSRR* by *ETS*  $V_{\text{max}}$ , i.e. without utilisation of *ETS* to carbon conversion factors, almost all the mesopelagic values would be lower than surface ones with averaged *CSRR* value of 0.34 and 0.29  $\text{fg C cell}^{-1}$  in the epi- and mesopelagic layers, respectively (data not shown). Although different from other reports from temperate seas (Placenti et al. 2018, Baltar et al. 2009), the *CSRR* in epipelagic water was higher than in the mesopelagic one, suggesting more actively respiring cells in the upper layers. Nevertheless, high *CSRR* values were found at stations where *TSI* was low, suggesting the importance of cell-specific respiration in oligotrophic conditions, in agreement with the findings of Baltar et al. (2015) for subantarctic waters. Conversely, *CSRR* in Summer 2014 was higher in the deeper layers than in the surface ones (Mistic et al. 2017). Nevertheless, high *CSRR* values were found at stations where *TSI* was low, which also corroborates the importance of prokaryotic respiration in the surface layer.

The cell-specific incorporation rate (*CSIR*) strictly reflected the distribution of *PHA* throughout the water column with the highest values in the surface to 50 m depth layer. The average *CSIR* was similar to that detected by Ducklow et al. (2001) and Pedrós-Alió et al. (2002) in the upper 50 m layer of the RS during Summer 1997 as well as in the Antarctic Peninsula, respectively. A decreased availability of organic carbon for synthesising new biomass could explain this finding (Baltar et al. 2015). The *CSIR*-temperature Spearman-rank relationships were positive in the photic layer and negative in the

aphotic one (data not shown). The positive correlation observed in the epipelagic layer amongst heterotrophic rates, *CHLa* and respiration, allowed us to consider a direct or indirect (previous exoenzymatic hydrolysis) flux of labile *DOC* from phytoplankton biomass and detritus towards the new prokaryotic biomass. In the XIX PNRA expedition (VLTP-2004 project), a mean of  $2.35 \mu\text{g C l}^{-1} \text{h}^{-1}$  potentially mobilised by leucine aminopeptidase +  $\beta$ -glucosidase activities, was detected in the photic layer off Victoria Land (Monticelli, personal communication). In the photic zone of Terra Nova Bay (RS), during summer 2000, the daily flow of C towards new prokaryotic biomass was equivalent to 0.2% of C, potentially mobilised by exoenzymatic activities (Monticelli et al. 2003).

Overall, in Summer 2005, the investigated area of the RS contributed in different ways to the epi- and mesopelagic layer carbon metabolism. *Per* sea-surface area, the autotrophic (by *C-CHLa*), prokaryotic (*PB*) and total standing stocks (*C-ATP*) amounted to 1545, 1681 and 4605  $\text{mg C m}^{-2}$ , respectively. The remaining heterotrophic component (*HB*) presumably accounted for a biomass of 1379  $\text{mg C m}^{-2}$ . The prokaryotic biomass appeared to be predominant in the mesopelagic layer with respect to the epipelagic one (depth integrated *PB* ratio epi/meso: 0.4). The entire heterotrophic production accounted for  $1.697 \text{ mg C m}^{-2} \text{ h}^{-1}$  with a similar weight in the epi- and mesopelagic layers (depth integrated *PHP* ratio epi/meso was 1.03). Respiration remineralised  $8.279 \text{ mg C m}^{-2} \text{ h}^{-1}$  with higher rates in the upper layers (depth integrated *CDPR* ratio epi/meso was 2.7).

## Conclusions

This study was carried out within a time series of research conducted since the nineties in the Ross Sea. Through their metabolic rates, microorganisms worked as regulators of the organic carbon transfer in the Ross Sea and impacted Antarctic biogeochemical cycles. In this experiment, highly variable microbial metabolism was detected at all stations and depth layers. At the same time, coherent metabolic patterns were detected using different, independent, methodological approaches. The distribution of plankton metabolism and organic matter degradation was mainly related to the general oligotrophic conditions occurring during Summer 2005. The processes of heterotrophic production, respiration and growth efficiency revealed relatively low levels of carbon remineralisation. Compared with other cruises carried out in the Ross Sea, dramatic changes were found on an inter-annual scale. Monitoring the heterotrophic microbial patterns in long term series is proving to be an interesting approach in furthering understanding of biogeochemical trends. In contexts such as the mooring sites of LTER-Italy, it needs to be better known due to the climate-change implication of Antarctic Ocean on the global scale.

## Acknowledgements

The research was funded by the XX Italian PNRA (National Programme of Antarctic Research, year 2004/05) expedition in the framework of the ABIOCLEAR project

(Antarctic BIOgeochemical cycles–Climatic and palEoclimAtic Reconstructions, coord. Dr. Mariangela Ravaioli of CNR-ISMAR, Institute of Marine Science) and received the financial support of P-ROSE project (Plankton biodiversity and functioning of the ROSS Sea Ecosystems in a changing southern ocean, funded by PNRA, National Programme of Antarctic Research, year 2016/18, coord. Prof. Olga Mangoni of CoNISMa, National Interuniversity Consortium for Marine Sciences) and of CEL-EBeR project (CDW effects on glacial melting and on bulk of Fe in the Western Ross Sea, funded by PNRA, National Programme of Antarctic Research, year 2016/18, coord. Prof. Paola Rivaro of University of Genoa). The authors thank all the staff of R/V *Italica* for the logistics help and support. PHA saturation curves analysis and time courses were fixed in a precedent project (Victoria Land Transect Project, VLTP-2004) funded by XIX PNRA Expedition. The T.T. Packard's contribution was supported by TIAA-CREF (USA) and Social Security (USA). The authors also thank the Editor and reviewers for their very useful comments and Mr. Alessandro Cosenza (ISP Institute of Polar Science) for figure processing.

## References

- Ahmed SI, Kenner RA, King FD (1976) Preservation of enzymic activity in marine plankton by low-temperature freezing. *Marine Chemistry* 4(2): 133–139. [https://doi.org/10.1016/0304-4203\(76\)90002-5](https://doi.org/10.1016/0304-4203(76)90002-5)
- Arístegui J, Montero MF (1995) The relationship between community respiration and ETS activity in the ocean. *Journal of Plankton Research* 17(7): 1563–1571. <https://doi.org/10.1093/plankt/17.7.1563>
- Azzaro M, La Ferla R, Azzaro F (2006) Microbial respiration in the aphotic zone of the Ross Sea (Antarctica). *Marine Chemistry* 99(1–4): 199–209. <https://doi.org/10.1016/j.marchem.2005.09.011>
- Azzaro M, La Ferla R, Maimone G, Monticelli LS, Zaccone R, Civitaresse G (2012) Prokaryotic dynamics and heterotrophic metabolism in a deep convection site of Eastern Mediterranean Sea (the Southern Adriatic Pit). *Continental Shelf Research* 44: 106–118. <https://doi.org/10.1016/j.csr.2011.07.011>
- Baltar F, Arístegui J, Sintés E, van Aken HM, Gasol JM, Herndl GJ (2009) Prokaryotic extracellular enzymatic activity in relation to biomass production and respiration in the meso and bathypelagic waters of the (sub) tropical Atlantic. *Environmental Microbiology* 11(8): 1998–2014. <https://doi.org/10.1111/j.1462-2920.2009.01922.x>
- Baltar F, Arístegui J, Gasol JM, Herndl GJ (2010) Prokaryotic carbon utilization in the dark ocean: growth efficiency, leucine-to-carbon conversion factors, and their relationship. *Aquatic Microbial Ecology* 60: 227–232. <https://doi.org/10.3354/ame01422>
- Baltar F, Stuck E, Morales S, Currie K (2015) Bacterioplankton carbon cycling along the Sub-tropical Frontal Zone off New Zealand. *Progress in Oceanography* 135: 168–175. <https://doi.org/10.1016/j.pocan.2015.05.019>
- Berg JM, Tymoczko JL, Stryer L (2002) *Biochemistry* Ed 5<sup>th</sup>. WH Freeman, New York.

- Biddanda BA, Ogdah M, Cotner J (2001) Dominance of bacterial metabolism in oligotrophic relative to eutrophic waters. *Limnology and Oceanography* 46(3): 730–739. <https://doi.org/10.4319/lo.2001.46.3.0730>
- Bird DF, Karl DM (1999) Uncoupling of bacteria and phytoplankton during the austral spring bloom in Gerlache Strait, Antarctic Peninsula. *Aquatic Microbial Ecology* 19: 13–27. <https://doi.org/10.3354/ame019013>
- Bratbak G (1985) Bacterial biovolume and biomass estimation. *Applied and Environmental Microbiology* 49: 1488–1493.
- Buitenhuis ET, Li WKW, Vaulot D, Lomas MW, Landry MR, Partensky F, Karl DM, Ulloa O, Campbell L, Jacquet S, Lantoiné F, Chavez F, Macias D, Gosselin M, McManus GB (2012) Picophytoplankton biomass distribution in the global ocean. *Earth System Science Data* 4(1): 37–46. <https://doi.org/10.5194/essd-4-37-2012>
- Cajal-Medrano R, Maske H (2005) Growth efficiency and respiration at different growth rates in glucose-limited chemostats with natural marine bacteria populations. *Aquatic Microbial Ecology* 38: 125–133. <https://doi.org/10.3354/ame038125>
- Carlson RE (1983) Discussion: “Using Differences Among Carlson’s Trophic State Index Values in Regional Water Quality Assessment” by Richard A. Osgood: *Water Resources Bulletin* 19(2): 307–308. <https://doi.org/10.1111/j.1752-1688.1983.tb05335.x>
- Carlson CA, Hansell DA (2003) The contribution of dissolved organic carbon and nitrogen to the biogeochemistry of the Ross Sea. In: Di Tullio G, Dunbar R (Eds) *Biogeochemistry of the Ross Sea*. AGU Antarctic Research Series Monograph 78: 123–142. <https://doi.org/10.1029/078ARS08>
- Carlson CA, Bates NR, Ducklow HW, Hansell DA (1999) Estimation of bacterial respiration and growth efficiency in the Ross Sea, Antarctica. *Aquatic Microbial Ecology* 19: 229–244. <https://doi.org/10.3354/ame019229>
- Carlson CA, Hansell DA, Peltzer ED, Smith Jr WO (2000) Stocks and dynamics of dissolved and particulate organic matter in the southern Ross Sea, Antarctica. *Deep-sea Research. Part II, Topical Studies in Oceanography* 47(15–16): 3201–3225. [https://doi.org/10.1016/S0967-0645\(00\)00065-5](https://doi.org/10.1016/S0967-0645(00)00065-5)
- Catalano G, Budillon G, La Ferla R, Povero P, Ravaioli M, Saggiomo V, Accornero A, Azzaro M, Carrada GC, Giglio F, Langone L, Mangoni O, Misic C, Modigh M (2006) The Ross Sea. A global budget of carbon and nitrogen in the Ross Sea (Southern Ocean). In: Liu KK, Atkinson L, Quinones R, Talaue-McManus L (Eds) *Carbon and Nutrient Fluxes in Continental Margins: A Global Synthesis*, Global Change, The IGBP Series, Springer, Berlin, 303–318.
- Celussi M, Cataletto B, Umami SF, Del Negro P (2009) Depth profiles of bacterioplankton assemblages and their activities in the Ross Sea. *Deep-sea Research. Part I, Oceanographic Research Papers* 56(12): 2193–2205. <https://doi.org/10.1016/j.dsr.2009.09.001>
- Constable AJ, Melbourne-Thomas J, Corney SP, Arrigo KR, Barbraud C, Barnes DKA, Bindoff NL, Boyd PW, Brandt A, Costa DP, Davidson AT, Ducklow HW, Emmerson L, Fukuchi M, Gutt J, Hindell MA, Hofmann EE, Hosie GW, Iida T, Jacob S, Johnston NM, Kawaguchi S, Kokubun N, Koubbi P, Lea M-A, Makhado A, Massom RA, Meiners K, Meredith MP, Murphy EJ, Nicol S, Reid K, Richerson K, Riddle MJ, Rintoul SR, Smith Jr WO, Southwell C, Stark JS, Sumner M, Swadling KM, Takahashi KT, Trathan PN, Welsford

- DC, Weimerskirch H, Westwood KJ, Wienecke BC, Wolf-Gladrow D, Wright SW, Xavier JC, Ziegler P (2014) Climate change and Southern Ocean ecosystems I: How changes in physical habitats directly affect marine biota. *Global Change Biology* 20(10): 3004–3025. <https://doi.org/10.1111/gcb.12623>
- Crisafi E, Azzaro M, Lo Giudice A, Michaud L, La Ferla R, Maugeri TL, De Domenico M, Azzaro F, Acosta Pomar MLC, Bruni V (2010) Microbiological characterization of a semi-enclosed sub-Antarctic environment: the Straits of Magellan. *Polar Biology* 33:1485–1504. <https://doi.org/10.1007/s00300-010-0836-6>
- del Giorgio PA, Cole JJ (1998) Bacterial growth yield efficiency in natural aquatic systems. *Annual Review of Ecology and Systematics* 29(1): 503–541. <https://doi.org/10.1146/annurev.ecolsys.29.1.503>
- del Giorgio PA, Williams P (2005) Respiration in aquatic ecosystems: history and background in: del Giorgio P, Williams P (Eds) *Respiration in Aquatic Ecosystems*. Oxford University Scholarship 1: 1–17. <https://doi.org/10.1093/acprof:oso/9780198527084.001.0001>
- del Giorgio PA, Condon R, Bouvier T, Longnecker K, Bouvier C, Sherr E, Gasol JM (2011) Coherent patterns in bacterial growth, growth efficiency, and leucine metabolism along a northeastern Pacific inshore-offshore transect. *Limnology and Oceanography* 56(1): 1–16. <https://doi.org/10.4319/lo.2011.56.1.0001>
- Deppler SL, Davidson AT (2017) Southern Ocean Phytoplankton in a Changing Climate. *Frontiers in Marine Science* 4(40): 1–28. <https://doi.org/10.3389/fmars.2017.00040>
- Dinasquet J, Ortega-Retuerta E, Lovejoy C, Obernosterer I (2018) Editorial: Microbiology of the Rapidly Changing Polar Environments. *Frontiers in Marine Science* 5: 154. <https://doi.org/10.3389/fmars.2018.00154>
- DiTullio GR, Grembleler JM, Arrigo KR, Lizotte MP, Robinson DH, Leventer A, Barry JP, VanWoert ML, Dunbar RB (2000) Rapid and early export of *Phaeocystis* Antarctica blooms in the Ross Sea, Antarctica. *Nature* 404(6778): 95–98. <https://doi.org/10.1038/35007061>
- Ducklow HW (2003) Seasonal production and bacterial utilization of DOC in the Ross Sea, Antarctica. In: DiTullio G, Dunbar R (Eds) *Biogeochemistry of the Ross Sea*, AGU Antarctic Research Series Monograph, vol. 78, 143–158. <https://doi.org/10.1029/078ARS09>
- Ducklow H, Carson C, Church M, Kirchman D, Smith D, Steward G (2001) The seasonal development of the bacterioplankton bloom in the Ross Sea, Antarctica 1994–1997. *Deep-sea Research. Part II, Topical Studies in Oceanography* 48(19–20): 4199–4221. [https://doi.org/10.1016/S0967-0645\(01\)00086-8](https://doi.org/10.1016/S0967-0645(01)00086-8)
- Dutta H, Dutta A (2016) The microbial aspect of climate change. *Energy, Ecology & Environment* 1(4): 209–232. <https://doi.org/10.1007/s40974-016-0034-7>
- Eichinger M, Sempéré R, Grégori G, Charrière B, Poggiale JC, Lefèvre D (2010) Increased bacterial growth efficiency with environmental variability: results from DOC degradation by bacteria in pure culture experiments. *Biogeosciences* 7: 1861–1876. <https://doi.org/10.5194/bg-7-1861-2010>
- Fabiano M, Povero P, Mistic C (2000) Spatial and temporal distribution of particulate organic matter in the Ross Sea. In: Faranda FM, Guglielmo L, Ianora A (Eds) *Ross Sea Ecology*. Springer-Verlag, Berlin Heidelberg, New York, 135–149. [https://doi.org/10.1007/978-3-642-59607-0\\_11](https://doi.org/10.1007/978-3-642-59607-0_11)

- Ferguson S (2010) ATP synthase: From sequence to ring size to the P/O ratio. *Proceedings of the National Academy of Sciences of the United States of America* 107(39): 16755–16756. <https://doi.org/10.1073/pnas.1012260107>
- Filella A, Baños I, Montero MF, Hernández-Hernández N, Rodríguez-Santos A, Ludwig A, Riebesell U, Arístegui J (2018) Plankton community respiration and ETS activity under variable CO<sub>2</sub> and nutrient fertilization during a mesocosm study in the subtropical North Atlantic. *Frontiers in Marine Science* 5: 310. <https://doi.org/10.3389/fmars.2018.00310>
- Fry JC (1990) 2 Direct methods and biomass estimation. *Methods in Microbiology* 22: 41–85. [https://doi.org/10.1016/S0580-9517\(08\)70239-3](https://doi.org/10.1016/S0580-9517(08)70239-3)
- Hammer Ø, Harper DAT, Ryan PD (2001) PAST: Paleontological Statistics Software Package for Education and Data Analysis. *Palaeontologia Electronica* 4(1): 9. [http://palaeo-electronica.org/2001\\_1/past/issue1\\_01.htm](http://palaeo-electronica.org/2001_1/past/issue1_01.htm)
- Hinkle PC (2005) P/O ratios of mitochondrial oxidative phosphorylation. *Biochimica et Biophysica Acta* 1706(1–2): 1–11. <https://doi.org/10.1016/j.bbabi.2004.09.004>
- Holm-Hansen O, Booth CR (1966) The measurement of adenosine triphosphate in the ocean and its ecological significance. *Limnology and Oceanography* 11(4): 510–519. <https://doi.org/10.4319/lo.1966.11.4.0510>
- Holm-Hansen O, Paerl HW (1972) The applicability of ATP determination for estimation of microbial biomass and metabolic activity. In: Melchiorri Santolini U, Hopton JH (Eds) *Detritus and its Role in Aquatic Ecosystems*. *Memorie dell'Istituto Italiano di Idrobiologia* 29: 149–168.
- Jiao N, Herndl GJ, Hansell DA, Benner R, Kattner G, Wilhelm SW, Kirchman DL, Weinbauer MG, Luo T, Chen F, Azam F (2010) Microbial production of recalcitrant dissolved organic matter: Long-term carbon storage in the global ocean. *Nature Reviews. Microbiology* 8(8): 593–599. <https://doi.org/10.1038/nrmicro2386>
- Karl DM (1980) Cellular Nucleotide Measurements and Applications in Microbial Ecology. *Microbiological Reviews* 44: 739–796.
- Karl DM (2014) Solar energy capture and transformation in the sea. *Elemental Science of the Anthropocene* 2: 1–6. <https://doi.org/10.12952/journal.elementa.000021>
- Kenner RA, Ahmed SI (1975) Measurements of electron transport activities in marine phytoplankton. *Marine Biology* 33(2): 119–127. <https://doi.org/10.1007/BF00390716>
- Khawwala S, Primeau F, Hall T (2009) Reconstruction of the history of anthropogenic CO<sub>2</sub> concentrations in the ocean. *Nature* 462: 346–349. <https://doi.org/10.1038/nature08526>
- Kjørboe T, Møhlenberg F, Hamburger K (1985) Bioenergetics of the planktonic copepod *Acartia tonsa*: relation between feeding, egg production and respiration, and composition of specific dynamic action. *Marine Ecology – Progress Series* 26: 85–97. <https://doi.org/10.3354/meps026085>
- Kirchman D (2001) Measuring bacterial biomass production and growth rates from leucine incorporation in natural aquatic environments. *Methods in Microbiology* 30: 227–236. [https://doi.org/10.1016/S0580-9517\(01\)30047-8](https://doi.org/10.1016/S0580-9517(01)30047-8)
- Kirchman D, K'nees E, Hobson R (1985) Leucine incorporation and its potential as a measure of protein synthesis by bacteria in natural aquatic systems. *Applied and Environment Microbiology* 49: 599–607.

- Koppelman R, Weikert H, Halsband-Lenk C, Jennerjahn T (2004) Mesozooplankton community respiration and its relation to particle flux in the oligotrophic eastern Mediterranean. *Global Biogeochemical Cycles* 18(1): 1039. <https://doi.org/10.1029/2003GB002121>
- La Ferla R, Azzaro M (2001a) Microbial respiration in the Levantine Sea: Evolution of the oxidative processes in relation to the main Mediterranean water masses. *Deep-sea Research. Part I, Oceanographic Research Papers* 48(10): 2147–2159. [https://doi.org/10.1016/S0967-0637\(01\)00009-7](https://doi.org/10.1016/S0967-0637(01)00009-7)
- La Ferla R, Azzaro M (2001b) Microplankton respiration (ETS) in two areas of the Northern Adriatic (Mediterranean Sea). *The New Microbiologica* 24(3): 265–271.
- La Ferla R, Azzaro F, Azzaro M, Caruso G, Decembrini F, Leonardi M, Maimone G, Monticelli LS, Raffa F, Santinelli C, Zaccone R, Ribera d'Alcalà M (2005) Microbial contribution to carbon biogeochemistry in the Central Mediterranean Sea: Variability of activities and biomass. *Journal of Marine Systems* 57(1–2): 146–166. <https://doi.org/10.1016/j.jmarsys.2005.05.001>
- La Ferla R, Azzaro M, Caruso G, Monticelli LS, Maimone G, Zaccone R, Packard TT (2010) Prokaryotic abundance and heterotrophic metabolism in the deep Mediterranean Sea. *Journal of Advances in Oceanography and Limnology* 1(1): 143–166. <https://doi.org/10.4081/aiol.2010.5298>
- La Ferla R, Maimone G, Lo Giudice A, Azzaro F, Cosenza A, Azzaro M (2015) Cell size and other phenotypic traits of prokaryotic cells in pelagic areas of the Ross Sea (Antarctica). *Hydrobiologia* 761: 181–194. <https://doi.org/10.1007/s10750-015-2426-7>
- Lancelot C (2007) Southern Ocean ecosystem: key for global climate. *Science & Technologies, Climate Change*. [www.sciencepoles.org](http://www.sciencepoles.org)
- Lane N (2006) Batteries not included. What can't bacteria do? *Nature* 441(7091): 274–277. <https://doi.org/10.1038/441274a>
- Langone L, Frignani M, Ravaioli M, Bianchi C (2000) Particle fluxes and biogeochemical processes in an area influenced by seasonal retreat of the ice margin (northwestern Ross Sea, Antarctica). *Journal of Marine Systems* 27(1–3): 221–234. [https://doi.org/10.1016/S0924-7963\(00\)00069-5](https://doi.org/10.1016/S0924-7963(00)00069-5)
- Langone L, Dunbar RB, Mucciarone DA, Ravaioli M, Meloni R, Nittrouer CA (2003) Rapid sinking of biogenic material during the late austral summer in the Ross Sea, Antarctica. In: DiTullio G, Dunbar R (Eds) *Biogeochemistry of the Ross Sea*, AGU Antarctic Research Series Monograph: 78: 221–234. <https://doi.org/10.1029/078ARS14>
- Lazzara L, Bianchi F, Falcucci M, Hull V, Modigh M, Ribera d'Alcalà M (1990) Pigmenti clorofilliani. *Nova Thalassia* 11: 207–223. <https://www.researchgate.net/publication/285881482>
- Lee S, Fuhrman A (1987) Relationship between biovolume and biomass of naturally derived bacterioplankton. *Applied and Environmental Microbiology* 53: 1298–1303. <https://aem.asm.org/content/53/6/1298>
- Legendre L, Rivkin RB, Weinbauer M, Guidi L, Uitz J (2015) The microbial carbon pump concept: Potential biogeochemical significance in the globally changing ocean. *Progress in Oceanography* 134: 432–450. <https://doi.org/10.1016/j.pocean.2015.01.008>
- Lemée R, Rochelle-Newall E, Van Wambeke F, Pizay M-D, Rinaldi P, Gattuso J-P (2002) Seasonal variation of bacterial production, respiration and growth efficiency in the open NW Mediterranean Sea. *Aquatic Microbial Ecology* 29: 227–237. <https://doi.org/10.3354/ame029227>

- Loferer-Krößbacher M, Klima J, Psenner R (1998) Determination of bacterial cell dry mass by transmission electron microscopy and densitometric image analysis. *Applied and Environmental Microbiology* 64: 688–694.
- Lotka A (1925) *Elements of physical biology*, Williams and Wilkins Company (Baltimore) 1–495.
- Manganelli M, Malfatti F, Samo TJ, Mitchell BG, Wang H, Azam F (2009) Major Role of Microbes in Carbon Fluxes during Austral Winter in the Southern Drake Passage. *PLoS ONE* 4(9): e6941. <https://doi.org/10.1371/journal.pone.0006941>
- Mangoni O, Saggiomo V, Bolinesi F, Margiotta F, Budillon G, Cotroneo Y, Misisic C, Rivaro P, Saggiomo M (2017) Phytoplankton blooms during austral summer in the Ross Sea, Antarctica: Driving factors and trophic implications. *PLoS One* 12(4): 1–23. <https://doi.org/10.1371/journal.pone.0176033>
- Marra J, Barber RT (2004) Phytoplankton and heterotrophic respiration in the surface layer of the ocean. *Geophysical Research Letters* 31(9, L09314): 1–4. <https://doi.org/10.1029/2004GL019664>
- Massana R, Gasol JP, Bjørnsen PK, Blackburn N, Hanström A, Hietanen S, Hygum BH, Kuopinen J, Pedrós-Alió C (1997) Measurement of bacterial size via image analysis of epifluorescence preparations: Description of an inexpensive system and solutions to some of the most common problems. *Scientia Marina* 61(3): 397–407. <http://hdl.handle.net/10261/28200>
- Mazuecos IP, Arístegui J, Vázquez-Domínguez E, Ortega-Retuerta E, Gasol JM, Reche I (2015) Temperature control of microbial respiration and growth efficiency in the mesopelagic zone of the South Atlantic and Indian Oceans. *Deep-sea Research. Part I, Oceanographic Research Papers* 95: 131–138. <https://doi.org/10.1016/j.dsr.2014.10.014>
- Minas HJ, Minas M, Packard TT (1986) Productivity in upwelling areas deduced from hydrographic and chemical fields 1. *Limnology and Oceanography* 31(6): 1182–1206. <https://doi.org/10.4319/lo.1986.31.6.1182>
- Misisic C, Covazzi Harriague A, Giglio F, La Ferla R, Rappazzo AC, Azzaro M (2017) Relationships between electron transport system (ETS) activity and particulate organic matter features in three areas of the Ross Sea (Antarctica). *Journal of Sea Research* 129: 42–52. <https://doi.org/10.1016/j.seares.2017.09.003>
- Monticelli LS, La Ferla R, Maimone G (2003) Dynamics of bacterioplankton activities after a summer phytoplankton bloom period in Terra Nova Bay. *Antarctic Science* 15(1): 85–93. <https://doi.org/10.1017/S0954102003001081>
- Moran L, Horton R, Scrimgeour K, Perry M (2012) *Principles of Biochemistry*, Prentice Hall (Saddle River NJ) 1–832. [www.pearsoned.co.uk](http://www.pearsoned.co.uk)
- Nelson DM, De Master DJ, Dunbar RB, Smith Jr WO (1996) Cycling of organic carbon and biogenic silica in the Southern Ocean: Estimates of water column and sedimentary fluxes on the Ross Sea continental shelf. *Journal of Geophysical Research* 101(C8): 519–532. <https://doi.org/10.1029/96JC01573>
- Ochoa S (1943) Efficiency of aerobic phosphorylation in cell-free heart extracts. *The Journal of Biological Chemistry* 151: 493–505. <https://www.jbc.org/content/151/2/493.full.pdf>
- Odum HT (1956) Primary production in flowing waters. *Limnology and Oceanography* 1(2): 102–117. <https://doi.org/10.4319/lo.1956.1.2.0102>

- Packard TT (1969) The estimation of the oxygen utilization rate in seawater from the activity of the respiratory electron transport system in plankton. PHD Thesis. University of Washington (Seattle). <https://www.researchgate.net/publication/34358782>
- Packard TT (1971) The measurement of respiratory electron transport activity in marine phytoplankton. *Journal of Marine Research* 29: 235–244. <https://www.researchgate.net/publication/285850981>
- Packard TT (1985) Measurement of electron transport activity of microplankton. In: Jannasch HW, Williams PJ- LeB (Eds) *Advances in Aquatic Microbiology*, vol. 3. Academic Press, New York, 207–261. <https://www.researchgate.net/publication/233843739>
- Packard TT (2017) Food for Thought: From Thoreau's woods to the Canary Islands: exploring ocean biogeochemistry through enzymology. *ICES Journal of Marine Science* 75(3): 912–922. <https://doi.org/10.1093/icesjms/fsx214>
- Packard TT, Christensen J (2004) Respiration and vertical carbon flux in the Gulf of Maine water column. *Journal of Marine Research* 62(1):93–115. <https://doi.org/10.1357/00222400460744636>
- Packard TT, Codispoti LA (2007) Respiration, mineralization, and biochemical properties of the particulate matter in the southern Nansen Basin water column in April 1981. *Deep-sea Research. Part I, Oceanographic Research Papers* 54(3): 403–414. <https://doi.org/10.1016/j.dsr.2006.12.008>
- Packard TT, Healy M, Richards F (1971) Vertical distribution of the activity of the respiratory electron transport system in marine plankton. *Limnology and Oceanography* 16(1): 60–70. <https://doi.org/10.4319/lo.1971.16.1.0060>
- Packard TT, Devol AH, King FD (1975) The effect of temperature on the respiratory electron transport system in marine plankton. *Deep-Sea Research and Oceanographic Abstracts* 22(4): 237–249. [https://doi.org/10.1016/0011-7471\(75\)90029-7](https://doi.org/10.1016/0011-7471(75)90029-7)
- Packard TT, Gómez M, Christensen J (2008) Fueling Western Mediterranean deep metabolism by deep water formation and shelf-slope cascading; evidence from 1981. In: Briand F (Ed.) *Dynamics of Mediterranean Deep Waters: CIESM Workshop Monographs* 38 (Monaco): 101–105. <https://www.researchgate.net/publication/259853127>
- Packard TT, Osma N, Fernández-Urruzola I, Codispoti LA, Christensen JP, Gómez M (2015) Peruvian upwelling plankton respiration: calculations of carbon flux, nutrient retention efficiency, and heterotrophic energy production. *Biogeosciences*, 12: 2641–2654. <https://doi.org/10.5194/bg-12-2641-2015>
- Pamatmat MM, Graf G, Bengtsson W, Novak CS (1981) Heat production, ATP concentration and electron transport activity of marine sediments. *Marine Ecology Progress Series* 4: 135–144. <https://doi.org/10.3354/meps004135>
- Pedrós-Alió C, Vaqué D, Guixa-Boiweureu N, Gasol JM (2002) Prokaryotic plankton biomass and heterotrophic production in western Antarctic waters during the 1995–1996 Austral summer. *Deep-sea Research. Part II, Topical Studies in Oceanography* 49(4–5): 805–825. [https://doi.org/10.1016/S0967-0645\(01\)00125-4](https://doi.org/10.1016/S0967-0645(01)00125-4)
- Placenti F, Azzaro M, Artale V, La Ferla R, Caruso G, Santinelli C, Maimone G, Monticelli LS, Quinci EM, Sprovieri M (2018) Biogeochemical patterns and microbial processes in the Eastern Mediterranean Deep Water of Ionian Sea. *Hydrobiologia* 815(1): 97–112. <https://doi.org/10.1007/s10750-018-3554-7>

- Pomeroy LR, Wiebe WJ (2001) Temperature and substrates as interactive limiting factors for marine heterotrophic bacteria. *Aquatic Microbial Ecology* 23: 187–204. <https://doi.org/10.3354/ame023187>
- Porter KG, Feig YS (1980) The use of DAPI for identifying and counting aquatic microflora. *Limnology and Oceanography* 25(5): 943–948. <https://doi.org/10.4319/lo.1980.25.5.0943>
- Procopio J, Fornés J (1997) Fluctuations of the proton-electromotive force across the inner mitochondrial membrane. *Physical Review. E* 55(5): 6285–6288. <https://doi.org/10.1103/PhysRevE.55.6285>
- Reinthal T, Herndl GJ (2005) Seasonal dynamics of bacterial growth efficiencies in relation to phytoplankton in the southern North Sea. *Aquatic Microbial Ecology* 39: 7–16. <https://doi.org/10.3354/ame039007>
- Rivkin RB, Legendre L (2001) Biogenic Carbon Cycling in the Upper Ocean: Effects of Microbial Respiration. *Science* 291(5512): 2398–2400. <https://doi.org/10.1126/science.291.5512.2398>
- Simon M, Azam E (1989) Protein content and protein synthesis rates of planktonic marine bacteria. *Marine Ecology Progress Series* 51: 201–213. <https://doi.org/10.3354/meps051201>
- Skjoldal HR, Båmstedt U (1977) Ecobiochemical studies on the deep-water pelagic community of Korsfjorden, Western Norway. Adenine nucleotides in zooplankton. *Marine Biology* 42(3): 197–211. <https://doi.org/10.1007/BF00397744>
- Smith DC, Azam E (1992) A simple, economical method for measuring bacterial protein synthesis in seawater using  $^3\text{H}$ -leucine. *Marine Microbial Food Webs* 6(2): 107–114. <https://www.gso.uri.edu/dcsmith/page3/page19/assets/smithazam92.PDF>
- Smith Jr WO, Carlson CA, Ducklow HW, Hansell DA (1998) Growth dynamics of Phaeocystis antarctica-dominated plankton assemblages from the Ross Sea. *Marine Ecology Progress Series* 168: 229–244. <https://doi.org/10.3354/meps168229>
- Smith WO, Ainley DA, Cattaneo-Vietti R (2007) Trophic interactions within the Ross Sea continental shelf ecosystem. *Philosophical Transactions of the Royal Society B Biological Sciences* 362 (1477): 95–111. <https://doi.org/10.1098/rstb.2006.1956>
- Steward FJ, Fritsen CH (2004) Bacteria-algae relationships in Antarctic sea ice. *Antarctic Science* 16(2): 143–156. <https://doi.org/10.1017/S0954102004001889>
- Sweeney C, Hansell DA, Carlson CA, Codispoti LA, Gordon LI, Marra J, Millero FJ, Smith WO, Takahashi T (2000) Biogeochemical regimes, net community production and carbon export in the Ross Sea, Antarctica. *Deep-sea Research. Part II, Topical Studies in Oceanography* 47(15–16): 3369–3394. [https://doi.org/10.1016/S0967-0645\(00\)00072-2](https://doi.org/10.1016/S0967-0645(00)00072-2)
- Takahashi T, Broecker WS, Langer S (1985) Redfield ratio based on chemical data from isopycnal surfaces. *Journal of Geophysical Research* 90: 6907–6924. <https://doi.org/10.1029/JC090iC04p06907>
- van Looij A, Riemann B (1993) Measurements of bacterial production in coastal marine environments using leucine: Application of a kinetic approach to correct for isotope dilution. *Marine Ecology Progress Series* 102: 97–104. <https://doi.org/10.3354/meps102097>
- Van Wambeke F, Christaki U, Giannakourou A, Moutin T, Souvemerzoglou K (2002) Longitudinal and vertical trends of bacterial limitation by phosphorus and carbon in the Mediterranean Sea. *Microbial Ecology* 43(1): 119–133. <https://doi.org/10.1007/s00248-001-0038-4>
- Vichi M, Coluccelli A, Ravaioli M, Giglio F, Langone L, Azzaro M, Azzaro F, La Ferla R, Catalano G, Cozzi S (2009) Modelling approach to the assessment of biogenic fluxes at a

selected Ross Sea site, Antarctica. *Ocean Science Discussions* 6: 1477–1512. <https://doi.org/10.5194/osd-6-1477-2009>

Young KD (2006) The selective value of bacterial shape. *Microbiology and molecular biology reviews* 70: 660–703. <https://doi.org/10.1128/MMBR.00001-06>

Zaccone R, Monticelli LS, Seritti A, Santinelli C, Azzaro M, Boldrin A, La Ferla R, Ribera d'Alcalà M (2003) Bacterial processes in the intermediate and deep layers of the Ionian Sea in winter 1999: Vertical profiles and their relationship to the different water masses. *Journal of Geophysical Research* 108(18): 1–11. <https://doi.org/10.1029/2002JC001625>

## Supplementary material 1

### Figure S1

Authors: Maurizio Azzaro, Theodore T. Packard, Luis Salvador Monticelli, Giovanna Maimone, Alessandro Ciro Rappazzo, Filippo Azzaro, Federica Grilli, Ermanno Crisafi, Rosabruna La Ferla

Data type: measurement

Explanation note: Isopleths of temperature and salinity at the sea-surface and at 200m depth in the Ross Sea during the ABIOCLEAR Project. The CTD stations are indicated by black dots.

Copyright notice: This dataset is made available under the Open Database License (<http://opendatacommons.org/licenses/odbl/1.0/>). The Open Database License (ODbL) is a license agreement intended to allow users to freely share, modify, and use this Dataset while maintaining this same freedom for others, provided that the original source and author(s) are credited.

Link: <https://doi.org/10.3897/natureconservation.34.30631.suppl1>

## Supplementary material 2

### Table S1

Authors: Maurizio Azzaro, Theodore T. Packard, Luis Salvador Monticelli, Giovanna Maimone, Alessandro Ciro Rappazzo, Filippo Azzaro, Federica Grilli, Ermanno Crisafi, Rosabruna La Ferla

Data type: parameters data

Explanation note: Acronyms of the studied parameters and link among some of them. The specific steps are described in the text.

Copyright notice: This dataset is made available under the Open Database License (<http://opendatacommons.org/licenses/odbl/1.0/>). The Open Database License (ODbL) is a license agreement intended to allow users to freely share, modify, and use this Dataset while maintaining this same freedom for others, provided that the original source and author(s) are credited.

Link: <https://doi.org/10.3897/natureconservation.34.30631.suppl2>

### Supplementary material 3

#### Table S2

Authors: Maurizio Azzaro, Theodore T. Packard, Luis Salvador Monticelli, Giovanna Maimone, Alessandro Ciro Rappazzo, Filippo Azzaro, Federica Grilli, Ermanno Crisafi, Rosabruna La Ferla

Data type: measurements

Explanation note: Trophic State Index (TSI) calculated from Chlorophyll a concentrations (CHLa in  $\text{mg m}^{-3}$ ) in the epipelagic layer and Adenosine Triphosphate (ATP in  $\text{ng l}^{-1}$ ) concentrations detected in the epi- and mesopelagic layers of each station.

Copyright notice: This dataset is made available under the Open Database License (<http://opendatacommons.org/licenses/odbl/1.0/>). The Open Database License (ODbL) is a license agreement intended to allow users to freely share, modify, and use this Dataset while maintaining this same freedom for others, provided that the original source and author(s) are credited.

Link: <https://doi.org/10.3897/natureconservation.34.30631.suppl3>

### Supplementary material 4

#### Table S3

Authors: Maurizio Azzaro, Theodore T. Packard, Luis Salvador Monticelli, Giovanna Maimone, Alessandro Ciro Rappazzo, Filippo Azzaro, Federica Grilli, Ermanno Crisafi, Rosabruna La Ferla

Data type: statistical data

Explanation note: Ranges, mean values and standard deviations of Cell Carbon Content (CCC as  $\text{fg C cell}^{-1}$ ) determined in each station in the epi- and mesopelagic layers.

Copyright notice: This dataset is made available under the Open Database License (<http://opendatacommons.org/licenses/odbl/1.0/>). The Open Database License (ODbL) is a license agreement intended to allow users to freely share, modify, and use this Dataset while maintaining this same freedom for others, provided that the original source and author(s) are credited.

Link: <https://doi.org/10.3897/natureconservation.34.30631.suppl4>

## **Supplementary material 5**

### **Table S4**

Authors: Maurizio Azzaro, Theodore T. Packard, Luis Salvador Monticelli, Giovanna Maimone, Alessandro Ciro Rappazzo, Filippo Azzaro, Federica Grilli, Ermanno Crisafi, Rosabruna La Ferla

Data type: measurement

Explanation note: Depth integrated data of prokaryotic (PB) and autotrophic (by C-CHLa) biomass, total standing stocks (C-ATP) and remaining heterotrophic biomass (HB); respiratory (CDPR) and prokaryotic heterotrophic production (PHP) rates in the epi-, mesopelagic layers and total water column.

Copyright notice: This dataset is made available under the Open Database License (<http://opendatacommons.org/licenses/odbl/1.0/>). The Open Database License (ODbL) is a license agreement intended to allow users to freely share, modify, and use this Dataset while maintaining this same freedom for others, provided that the original source and author(s) are credited.

Link: <https://doi.org/10.3897/natureconservation.34.30631.suppl5>